Mon. Not. R. Astron. Soc. **355,** 769–784 (2004) doi:10.1111/j.1365-2966.2004.08354.x

Galaxy groups in the Two-degree Field Galaxy Redshift Survey: the luminous content of the groups

V. R. Eke,[1⋆] Carlos S. Frenk,[1] Carlton M. Baugh,[1] Shaun Cole,[1] Peder Norberg,[2] John A. Peacock,[3] Ivan K. Baldry,[4] Joss Bland-Hawthorn,[5] Terry Bridges,[5] Russell Cannon,[5] Matthew Colless,[6] Chris Collins,[7] Warrick Couch,[8] Gavin Dalton,[9,10] Roberto de Propris,[8] Simon P. Driver,[6] George Efstathiou,[11] Richard S. Ellis,[12] Karl Glazebrook,[4] Carole A. Jackson,[6] Ofer Lahav,[11,13] Ian Lewis,[9] Stuart Lumsden,[14] Steve J. Maddox,[15] Darren Madgwick,[16] Bruce A. Peterson,[6] Will Sutherland[10] and Keith Taylor[12] (the 2dFGRS Team)

[1]*Department of Physics, University of Durham, South Road, Durham DH1 3LE*
[2]*ETHZ Institut für Astronomie, HPF G3.1, ETH Hönggerberg, CH-8093 Zürich, Switzerland*
[3]*Institute for Astronomy, University of Edinburgh, Royal Observatory, Blackford Hill, Edinburgh EH9 3HJ*
[4]*Department of Physics & Astronomy, Johns Hopkins University, Baltimore, MD 21218-2686, USA*
[5]*Anglo-Australian Observatory, PO Box 296, Epping, NSW 2121, Australia*
[6]*Research School of Astronomy and Astrophysics, The Australian National University, Canberra, ACT 2611, Australia*
[7]*Astrophysics Research Institute, Liverpool John Moores University, 12 Quays House, Birkenhead L14 1LD*
[8]*Department of Astrophysics, University of New South Wales, Sydney, NSW 2052, Australia*
[9]*Department of Physics, University of Oxford, Keble Road, Oxford OX1 3RH*
[10]*Rutherford Appleton Laboratory, Chilton, Didcot OX11 0QX*
[11]*Institute of Astronomy, University of Cambridge, Madingley Road, Cambridge CB3 0HA*
[12]*Department of Astronomy, California Institute of Technology, Pasadena, CA 91125, USA*
[13]*Department of Physics and Astronomy, University College London, Gower Street, London WC1E 6BT*
[14]*Department of Physics, University of Leeds, Woodhouse Lane, Leeds LS2 9JT*
[15]*School of Physics & Astronomy, University of Nottingham, Nottingham NG7 2RD*
[16]*Department of Astronomy, University of California, Berkeley, CA 92720, USA*

Accepted 2004 August 23. Received 2004 August 10; in original form 2004 February 13

ABSTRACT

The Two-degree Field Galaxy Redshift Survey (2dFGRS) Percolation-Inferred Galaxy Group (2PIGG) catalogue of ∼29 000 objects is used to study the luminous content of galaxy systems of various sizes. Mock galaxy catalogues constructed from cosmological simulations are used to gauge the accuracy with which intrinsic group properties can be recovered. It is found that a Schechter function is a reasonable fit to the galaxy luminosity functions in groups of different mass in the real data, and that the characteristic luminosity $L_\star$ is slightly larger for more massive groups. However, the mock data show that the shape of the recovered luminosity function is expected to differ from the true shape, and this must be allowed for when interpreting the data. Luminosity function results are presented in both the $b_{\rm J}$ and $r_{\rm F}$ wavebands. The variation of the halo mass-to-light ratio, Υ, with group size is studied in both of these wavebands. A robust trend of increasing Υ with increasing group luminosity is found in the 2PIGG data. Going from groups with $b_{\rm J}$ luminosities equal to $10^{10}\,h^{-2}\ {\rm L}_\odot$ to those 100 times more luminous, the typical $b_{\rm J}$-band mass-to-light ratio increases by a factor of 5, whereas the $r_{\rm F}$-band mass-to-light ratio grows by a factor of 3.5. These trends agree well with the predictions of the simulations which also predict a minimum in the mass-to-light ratio on a scale roughly corresponding to the Local Group. The data indicate that if such a minimum exists, then it must occur at

⋆E-mail: v.r.eke@durham.ac.uk

© 2004 RAS

Downloaded from https://academic.oup.com/mnras/article-abstract/355/3/769/952880 by California Institute of Technology user on 19 May 2020

$L \lesssim 10^{10}\,h^{-2}\,\mathrm{L}_{\odot}$, below the range accurately probed by the 2PIGG catalogue. According to the mock data, the b_{J} mass-to-light ratios of the largest groups are expected to be approximately 1.1 times the global value. Assuming that this correction applies to the real data, the mean b_{J} luminosity density of the Universe yields an estimate of $\Omega_{\mathrm{m}} = 0.26 \pm 0.03$ (statistical error only). Various possible sources of systematic error are considered, with the conclusion that these could affect the estimate of Ω_{m} by a few tens of per cent.

Key words: galaxies: clusters: general – galaxies: haloes – large-scale structure of Universe.

Downloaded from https://academic.oup.com/mnras/article-abstract/355/3/769/952880 by California Institute of Technology user on 19 May 2020

1 INTRODUCTION

The distribution of galaxy luminosities, along with their mass-to-light ratios and spatial distribution, represent key observations that should be explained by theories of galaxy formation. In the Lambda cold dark matter (ΛCDM) model of structure formation, these broad brush empirical characterizations of the galaxy population result from a complicated interplay between the lumpy growth and coalescence of dark matter haloes and the radiative cooling, star formation and feedback associated with baryons within these clumps. Not only are the galaxies signposts to locating the underlying overdensities in the dark matter distribution, their properties also provide a systematic record of the processes that have taken place in those haloes and their progenitors. To develop a deeper understanding of the impact of these various processes, it is helpful to break down the global constraints referred to above and to consider their variation with halo mass.

The determination of the luminosity function of galaxies has received much observational effort (e.g. Blanton et al. 2001, 2003; Cole et al. 2001; Kochanek et al. 2001; Norberg et al. 2002), and recently there have been suggestions that the distribution of galaxy luminosities varies between rich cluster environments and low-density regions (e.g. Christlein 2000; Zabludoff & Mulchaey 2000; Balogh et al. 2001; de Propris et al. 2003). Furthermore, some authors find evidence that a Schechter function does not describe the galaxy luminosity function well in groups and clusters because of an excess of bright galaxies (e.g. Sandage, Binggeli & Tammann 1985; Ferguson & Sandage 1991; Smith, Driver & Phillipps 1997; Trentham & Tully 2002; Christlein & Zabludoff 2003). While these empirical results are intriguing, a systematic study with a large set of homogenous groups would add welcome weight to these findings. What should one expect to find? This question has been addressed using semi-analytical prescriptions (White & Frenk 1991; Kauffmann, White & Guiderdoni 1993; Diaferio et al. 1999; Benson et al. 2003b). These techniques provide a physically motivated *ab initio* procedure for calculating the properties of galaxy populations, which can be compared with the real Universe in order to constrain the physical processes and their implementation within the models. Both Diaferio et al. and Benson et al. find that the galaxy luminosity functions within haloes of different mass are not well described by Schechter functions. Instead, they have an excess in the abundance at the bright end which arises from the different processes that are important for the growth of the large central galaxy relative to the other galaxies in the haloes (the satellites). In smaller haloes, where a larger fraction of the group luminosity is typically locked up in the central galaxy, this produces a more prominent deviation from a Schechter function at the bright end of the galaxy luminosity function of the group. Furthermore, the luminosity at which this 'central galaxy bump' occurs, increases with halo mass. Testing the predictions from these models represents an opportunity to learn about aspects of galaxy formation.

The mass-to-light ratios (Υ) of groups represent another important clue, the light-to-mass ratio essentially reflecting the efficiency with which stars are formed within haloes of different mass. In large haloes this should be determined by the rate of gas cooling, whereas in small haloes other factors that cause energy to be injected into the halo gas become effective at disrupting the formation of stars. The prediction of semi-analytical models is that mass should be converted most efficiently into optical light in haloes of mass $\sim 10^{12}\,h^{-1}\,\mathrm{M}_{\odot}$ (White & Frenk 1991; Kauffmann et al. 1999; Benson et al. 2000). One way in which this can be tested is to take a theoretically motivated mass function and match haloes with galaxy groups of the same abundance as inferred from an empirically determined group luminosity function. This reveals the variation of the typical Υ with mass. Qualitatively, Marinoni & Hudson (2002) find a trend similar to that predicted by semi-analytical models, namely a minimum Υ at intermediate masses of $\sim 10^{12}\,h^{-1}\ \mathrm{M}_{\odot}$. Observationally, there have been many studies that have directly measured Υ for clusters and large groups of galaxies in various wavebands (R, Carlberg et al. 1996, 2001; Tucker et al. 2000; V, Schaeffer et al. 1993; David, Jones & Forman 1995; Cirimele, Nesci & Trèvese 1997; Hradecky et al. 2000; B, Ramella, Pisani & Geller 1997; Adami et al. 1998; Girardi et al. 2000, 2002; Sanderson & Ponman 2003; Tully 2004). Some studies suggest that the mass-to-light ratio is larger in bigger systems, whereas other studies find no significant variation.

In addition to the direct relevance of the mass-to-light ratio and its dependence on halo mass for studies of galaxy formation, Υ is an important quantity to measure as it provides one of the traditional ways to estimate the mean matter density of the Universe (e.g. Carlberg et al. 1996). This requires an assumption concerning the relation between the mass-to-light ratio of the groups or clusters and the mean cosmic value. Traditionally, it has been assumed that the value of Υ for the most massive clusters is representative of the universal mean, although for a long time this assumption was challenged in biased models of galaxy formation (Davis et al. 1985). At any rate, the value of Υ for clusters, together with an appropriate assumption concerning its universality and knowledge of the total galaxy luminosity density allows a simple estimate of the mean mass density for the Universe.

The construction of the two-degree Field Galaxy Redshift Survey (2dFGRS) Percolation-Inferred Galaxy Group (2PIGG) catalogue (Eke et al. 2004) from the 2dFGRS (Colless et al. 2001, 2003) facilitates a direct calculation of the galaxy content in a large sample of homogenous groups. The purpose of this paper is to report the results of a decomposition, by group size, of the luminosity functions of galaxies within groups, and the group mass-to-light ratio. Mock catalogues constructed from cosmological simulations are employed as a guide to the accuracy with which these

quantities can be inferred from the 2PIGG sample. This is a vital step in the comparison of a model prediction with the observational results.

Section 2 contains a brief description of the group catalogue and a quantitative study of its reliability. In Section 3 the luminosity functions of galaxies within groups is shown for different halo masses. The variation of total halo mass-to-light ratio with halo size is investigated in Section 4.

2 INFERRED GROUP PROPERTIES

A detailed description of the construction of the mock catalogues, and the group-finding algorithm applied both to these and the real 2dFGRS was given by Eke et al. (2004). Briefly, three different ΛCDM dark matter N-body simulations were used. They had (L, $N_{\rm p}$, σ_8) = (154, 288^3, 0.7), (250, 500^3, 0.8) and (141, 256^3, 0.9), where L is the side of the computational cube in h^{-1} Mpc, $N_{\rm p}$ is the number of particles and σ_8 is the rms linear density fluctuation in $8\,h^{-1}$ Mpc spheres. (The last of these is the GIF simulation described in Jenkins et al. 1998). The semi-analytical model of galaxy formation described by Cole et al. (2000) was implemented in the simulations to create populations of model galaxies where the observable properties are given by the model.

Although the semi-analytical model produces a galaxy luminosity function which is quite similar to that in the 2dFGRS, a small rescaling of the $b_{\rm J}$ luminosities was applied, to produce a model luminosity function which was identical to that in the 2dFGRS. Mock 2dFGRS catalogues were then constructed with the same geometry and position-dependent flux limit as the 2dFGRS, and samples of groups were selected by applying exactly the same cluster-finding algorithm used to generate the 2PIGG catalogue. The effects of fibre collisions in the 2dFGRS have been included in some mock catalogues. However, they have no significant impact on the quantities studied here, so the mock catalogues presented do actually include close pairs of galaxies that would not always be present in the real 2dFGRS. The $r_{\rm F}$-band magnitudes were rescaled in the same way as those in the $b_{\rm J}$ band, preserving the semi-analytical galaxy colours. Unlike in the $b_{\rm J}$ band, the resulting galaxy $r_{\rm F}$-band luminosity functions for the mock and 2dFGRS catalogues are thus not identical, as detailed in the Appendix.

Here, the focus is on describing the pertinent group properties and quantifying the accuracy with which they are inferred. The latter relies entirely on the mock catalogues, for which the true properties of the haloes hosting the groups are known in the parent simulation.

As described by Eke et al. (2004), the group mass is inferred dynamically according to

$$M = A\frac{\sigma^2 r}{G}, \tag{2.1}$$

where $A = 5.0$, σ is the one-dimensional velocity dispersion, calculated using the gapper algorithm (Beers, Flynn & Gebhardt 1990) and removing 85 km s^{-1} in quadrature to account for redshift measurement errors, and r is the rms projected separation of galaxies from the group centre, assuming an $\Omega_{\rm m} = 0.3$, $\Omega_\Lambda = 0.7$ cosmological model. The value of A has been chosen by reference to mock catalogues in which galaxies trace the dark matter within each halo, apart from a 'central' galaxy placed at the halo centre of mass. If real galaxies trace real haloes differently from those in the mock catalogues, then this value of A might not be appropriate. For instance, either a different spatial distribution or some velocity bias could give rise to a systematic error in the mass estimates of real groups. There is some evidence from gravitational lensing studies that bright galaxies do indeed trace the mass, at least in rich clusters (Hoekstra et al. 2002; Kneib et al. 2003). However, these current observational constraints are not yet sufficiently stringent that the effective value of A can be empirically justified to better than a few tens of per cent. This level of systematic uncertainty in the estimated masses is the main potential source of error in this paper.

2.1 Calculating group luminosities

In order to calculate the total group luminosity, it is necessary to correct for the incompleteness in the 2dFGRS. When finding the groups, galaxies from the parent catalogue that have no measured redshift have their weights redistributed equally to the nearest 10 projected galaxies with measured redshifts, and these galaxies are assigned a larger linking volume accordingly. As the sets of galaxies with and without redshifts are random subsamples (in terms of the intrinsic galaxy properties) of the same underlying galaxy population (ignoring the small level of flux-dependent redshift incompleteness), the incompleteness can simply be taken into account by totalling the observed group $b_{\rm J}$ luminosity according to

$$L_{{\rm obs},b_{\rm J}} = \sum_i^{n_{\rm gal}} w_i L_{i,b_{\rm J}}, \tag{2.2}$$

where the sum extends over the $n_{\rm gal}$ galaxies in the group with their individual weights, w_i. The total group luminosity is then estimated by including the contribution from galaxies below the luminosity limit, $L_{\rm min}$, at the redshift of the group. The extrapolation to zero galaxy luminosity is performed assuming that a Schechter function describes the number of galaxies as a function of luminosity. Given that the Schechter function is

$$\phi(L)\,{\rm d}L = \phi_*\left(\frac{L}{L_*}\right)^\alpha \exp\left(-\frac{L}{L_*}\right)\frac{{\rm d}L}{L_*}, \tag{2.3}$$

this operation merely involves dividing the observed luminosity by the incomplete Gamma function $\Gamma(\alpha+2,\, L_{\rm min}/L_*)/\Gamma(\alpha+2)$. In practice, a small correction is also applied because galaxies with fluxes corresponding to $b_{\rm J} < 14$ have been removed from the redshift catalogue. This bright flux limit only makes a perceptible difference for a few very local groups. These calculations require the additional information that $\mathrm{M}_\odot = 5.33$ in the $b_{\rm J}$ band and the adopted ($k+e$)-correction is similar to that of Norberg et al. (2002),

$$k + e = \frac{z + 6z^2}{1 + 8.9z^{5/2}}. \tag{2.4}$$

The global (M_*, α) = (−19.725, −1.18) values are used to extrapolate to the total luminosity for all groups. These values differ slightly from those of Norberg et al. (2002) as they have been derived from the recalibrated 2dFGRS (Colless et al. 2003). Using a global Schechter function to add in the luminosity from galaxies beneath the survey flux limit is only appropriate if the luminosity function shapes are similar in groups of different size. This can be tested directly using the data, and is performed in Section 3. In practice, a halo mass-dependent extrapolation changes the inferred luminosities by no more than ∼10 per cent.

At $z > 0.12$, the fraction of the total group luminosity that is actually observed drops below a half. Additionally, according to the mock catalogues, the amount of contamination of group membership increases at these higher redshifts. Thus, in all of what follows, only groups at $z < 0.12$ will be considered. This provides a large number of well-sampled groups with a range of masses up to $\sim 10^{15}\,h^{-1}\ \mathrm{M}_\odot$. The number of groups as a function of mass and luminosity is shown in Figs 1 and 2 for both the mock and

Downloaded from https://academic.oup.com/mnras/article-abstract/355/3/769/952880 by California Institute of Technology user on 19 May 2020

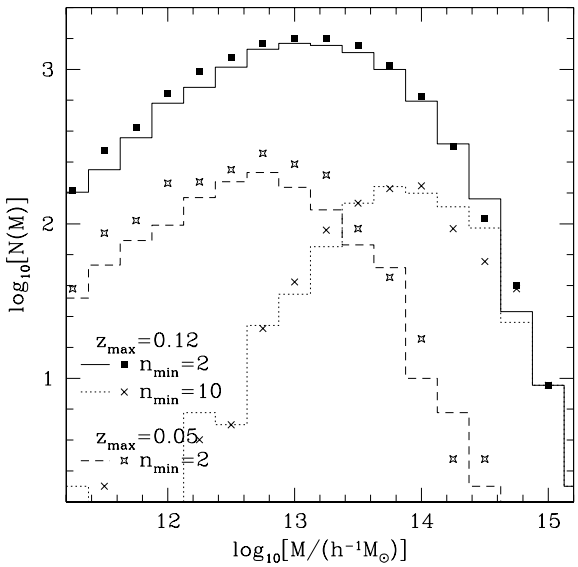

Figure 1. The number of groups at $z < 0.12$ and $z < 0.05$ as a function of the group dynamical mass, M. Solid and dotted lines correspond to the mock catalogues with $z_{\rm max} = 0.12$ and $n_{\rm min} = 2$ and 10, respectively. Filled squares and crosses are similar for the 2PIGG catalogue. The dashed line denotes $z_{\rm max} = 0.05$ and $n_{\rm min} = 2$, and the corresponding result from the real catalogue is shown with stars.

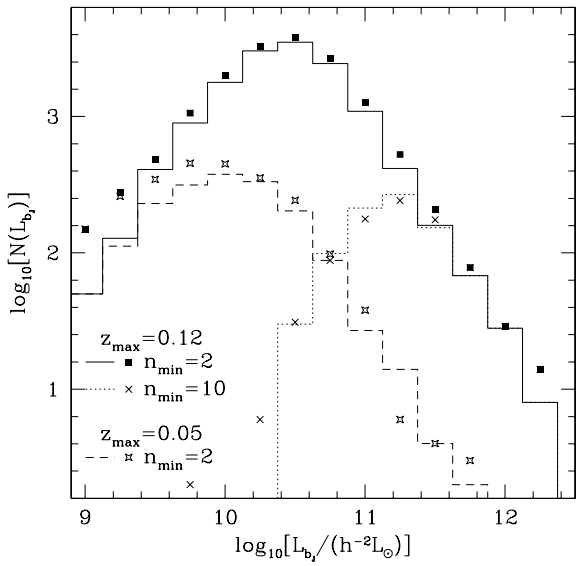

Figure 2. The number of groups as a function of the total group $b_{\rm J}$-band luminosity, $L_{b_{\rm J}}$. The lines and symbols have the same meaning as in Fig. 1.

real catalogues, choosing the minimum group membership to be $n_{\rm min} = 2$ or 10. Distributions of $n_{\rm min} = 2$ groups at $z < 0.05$ are also shown in these figures. The mock and real catalogues yield broadly similar numbers of groups with similar masses and luminosities. There is a slight deficit of groups in the mock catalogue relative to the 2PIGG data. This originates from the lack of low-luminosity galaxies included at $z < 0.04$, as described by Eke et al. (2004).

Complications arise when using the SuperCOSMOS (Hambly, Irwin & MacGillivray 2001) $r_{\rm F}$-band data because the 2dFGRS is a $b_{\rm J}$-selected survey. Different depths in the red luminosity function are thus probed for galaxies of different spectral types. Rather than dealing with the explicit dependence of the luminosity function on colour, the sample was re-cut to a conservative $r_{\rm F}$ limit such that almost all 2dFGRS galaxies can be detected to the same red luminosity at a given redshift. This issue is discussed in detail in the Appendix, which justifies re-cutting the sample at a local limit of $r_{\rm F,lim} = b_{\rm J,lim} - 1.5$.

2.2 The accuracy of measured halo properties

The typical redshift error in the 2dFGRS of $\sim$85 km s^{-1} (Colless et al. 2001) will lead to small-mass haloes having considerable errors in their estimated velocity dispersions and hence masses. For instance, $\sigma = 85$ km s^{-1} and $r = 100\ h^{-1}$ kpc correspond to a mass of approximately $10^{12}\,h^{-1}$ M$_\odot$. In order to interpret the results in the following sections, it is important to quantify the degree of uncertainty in the estimated halo masses and luminosities and how this varies with properties such as the number of member galaxies, $n_{\rm gal}$, or halo luminosity.

The 'accuracy' with which a halo property is estimated is defined as a logarithmic measure of the error in the property:

$$\text{accuracy} \equiv \log_{10}\left(\frac{y_{\rm recovered}}{y_{\rm true}}\right), \tag{2.5}$$

where y can denote mass, $b_{\rm J}$ or $r_{\rm F}$ luminosity, 'true' corresponds to the model from which the mock is constructed and 'recovered' stands for what is measured from the mock catalogue. Figs 3 and 4 show how the median accuracies, and the 16th and 84th percentiles (as opposed to the mean $\pm\,1\sigma$), vary as functions of $n_{\rm gal}$ and $L_{b_{\rm J}}$, respectively. Fig. 3 shows that the spread in mass accuracies becomes very large when the number of group members is less than 10. For more populated groups, the median accuracy is approximately zero, meaning that the typical inferred mass is unbiased. The luminosities are typically overestimated by a few tens of per cent even for well-populated groups, but they can still be relatively well determined for binaries. As the redshift space volumes of clusters also contain galaxies not in the same real space haloes, a degree of contamination is inevitable if all true cluster members are to be recovered. This is discussed by Eke et al. (2004), and it is these interlopers that are responsible for the typical overestimation of the luminosities.

From Fig. 3, one can infer that the measured group luminosity is a better quantity than the measured dynamical mass for ranking the groups in order of size, because it is still well determined for the less populated systems. Note that the accuracy of $r_{\rm F}$ luminosities has a larger spread than that in the $b_{\rm J}$ band. This is the result of using fewer galaxies to calculate the $r_{\rm F}$ luminosity, so the Schechter function correction for unobserved galaxies is slightly larger in the $r_{\rm F}$ than in the $b_{\rm J}$ band. Similar trends are visible in Fig. 4, where the distributions of accuracies are shown as a function of group luminosity for two different values of $n_{\rm min}$. At low group luminosity, particularly for $n_{\rm min} = 2$, the halo masses become increasingly overestimated and poorly determined due to the impact of the 2dFGRS redshift errors and contamination. Also apparent is a tail of underestimated group $r_{\rm F}$ luminosities at low-$b_{\rm J}$ group luminosity. These are binary groups with no members that satisfy the adopted flux limits, and are thus assigned zero $r_{\rm F}$-band luminosity.

Armed with this quantitative understanding of the group catalogue, and the systematic uncertainties resulting from the group-finding procedure, it is now appropriate to see what information can be extracted concerning the galaxy populations in different sizes of halo.

Downloaded from https://academic.oup.com/mnras/article-abstract/355/3/769/952880 by California Institute of Technology user on 19 May 2020

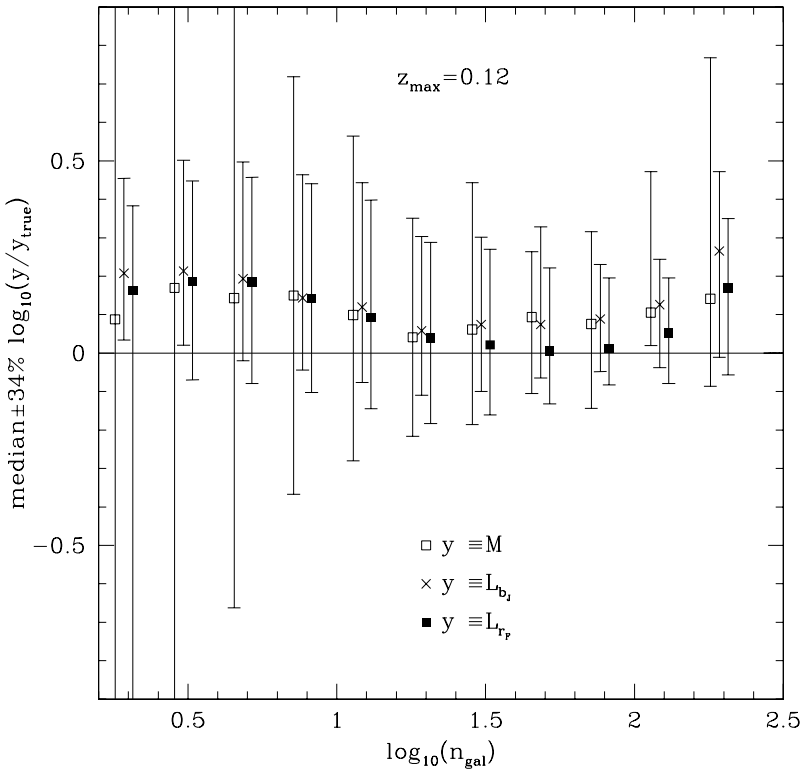

Figure 3. The median accuracies (symbols) ±34 percentiles (error bars) of the inferred group properties as a function of the number of galaxies in a group, $n_{\rm gal}$. All groups with $z \leqslant 0.12$ are included. The symbols correspond to the following group properties: $y = M$ (open squares), L_{b_J} (crosses) and L_{r_F} (filled squares). The points have been slightly displaced either side of the true bin values for clarity.

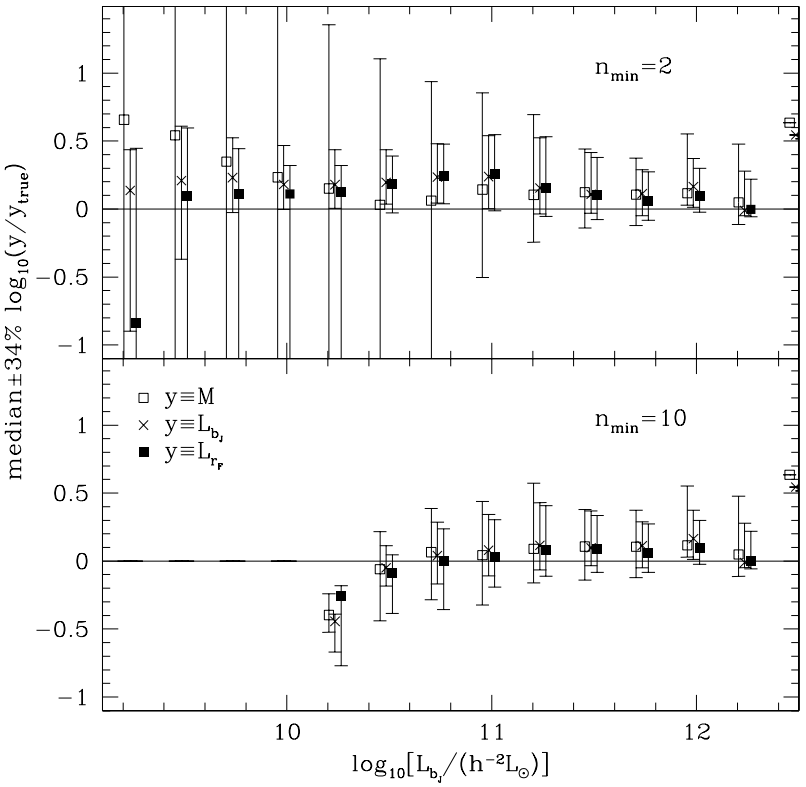

Figure 4. The median accuracies (symbols) ±34 percentiles of the inferred group properties as a function of the inferred group luminosity, L_{b_J}. In the top panel, $n_{\rm min} = 2$ and, in the bottom panel, $n_{\rm min} = 10$. Each bundle of three symbols has the following order from left to right: $y = M$, L_{b_J} and L_{r_F}. The points have been slightly displaced either side of the true bin values for clarity.

Downloaded from https://academic.oup.com/mnras/article-abstract/355/3/769/952880 by California Institute of Technology user on 19 May 2020

3 GALAXY LUMINOSITY FUNCTIONS WITHIN GROUPS

This section addresses first the issue of how well the galaxy luminosity function in haloes of different mass can be recovered from the mock catalogues and, secondly, the determination of these functions for the real data. These galaxy luminosity functions are also a necessary ingredient for calculating total group luminosities, because of the need to extrapolate the detected luminosity below the flux limit of the survey. In calculating the space density of galaxies, a $1/V_{\rm max}$ estimator has been applied to each galaxy. The variable flux limit across the survey has been taken into account. Dynamically inferred group masses, calculated according to equation (2.1), have been used to split the total sample into different classes.

3.1 $b_{\rm J}$-band results

Sets of mock catalogues have been constructed from two different semi-analytical models of galaxy formation applied to the same N-body simulations. Both of these models are based on the general scheme developed by Cole et al. (2000), but they treat certain physical processes in different ways. The first model, described by Benson et al. (2002), is very similar to the original Cole et al. model except that it includes detailed treatments of photoionization of the intergalactic medium at high redshift and of the dynamics of satellites in haloes. This model will be referred to as the 'bumpy' model because of the shape it predicts for the luminosity function of galaxies in clusters. A bump is created at high galaxy luminosity as a result of the treatment of the central cluster galaxy. Benson et al. (2003b) used this bumpy model to predict the luminosity function of galaxies in haloes of different mass. The second model comes from Benson et al. (2003a) and will be referred to as the 'superwind' model. This has a baryon fraction twice as high as that assumed by Cole et al., in accordance with recent determinations, and includes a treatment of superwinds. These suppress the growth of the overly bright galaxies, which otherwise tend to form in high baryon fraction models.

Fig. 5 shows galaxy luminosity functions in groups of different mass in both the semi-analytical models of galaxy formation. The solid lines correspond to the bumpy model, while the dashed lines correspond to the superwind model. The suppression of bright central galaxies in the superwind model is apparent in the middle and right-hand panels, which show the galaxy luminosity functions within groups of mass $M \sim 10^{14}$ and $\sim 10^{15}\,h^{-1}\ {\rm M}_{\odot}$, respectively. It is clear that the detailed shapes of the galaxy luminosity functions in groups depend upon the assumptions that go into making a semi-analytical model. These data can thus be used to test the models. In what follows, the bumpy mock catalogues will be shown unless otherwise stated.

In order to recover faithfully both the amplitude and shape of the galaxy luminosity function in groups of different mass, it is helpful to adopt separate values of $n_{\rm min}$ and $z_{\rm max}$ for the various group samples. For instance, clusters that should contribute to the highest-mass bin will have large numbers of members and be detectable to higher redshifts compared with the smaller groups. Thus, the following empirical choices of $(n_{\rm min}, z_{\rm max})$ were made for the 10^{13}, 10^{14} and $10^{15}\,h^{-1}\ {\rm M}_{\odot}$ samples, respectively: [(3, 0.08), (10, 0.12), (80, 0.12)]. These will be used throughout this section.

The results of these selections can be seen in Fig. 6, which shows the semi-analytical model luminosity functions in the simulations from which the mock catalogues were created, the luminosity functions actually recovered from the mock catalogues, and the luminosity functions estimated from the 2PIGG sample for the same values of $n_{\rm min}$ and $z_{\rm max}$. While the theoretical luminosity functions in the simulations from which the mock catalogues were made differ substantially from Schechter functions, the bumps have been largely smeared out in the mock recovered luminosity functions, which now better resemble Schechter functions. This smearing is predominantly the result of contaminating galaxies contributing to haloes with inappropriate masses and homogenizing the samples. Note that the original bumps occur at luminosities that vary with halo mass. There is a tentative bump detection in the two higher-mass group samples. This excess of luminous galaxies is sufficient to render the Schechter function a bad fit, although it does provide a good description of the results for the $M \sim 10^{13}\,h^{-1}\ {\rm M}_{\odot}$ groups. Overall, however, apart from the smearing out of the central galaxy bumps, the shapes and amplitudes of the group galaxy luminosity functions are recovered well from the mock catalogue.

Having determined the efficiency with which group mass-dependent galaxy luminosity functions are recovered, it is now appropriate to consider the real data. The 2PIGG results are shown by the points in Fig. 6. Error bars are the Poisson errors on the number of groups contributing galaxies to each luminosity bin. In almost all

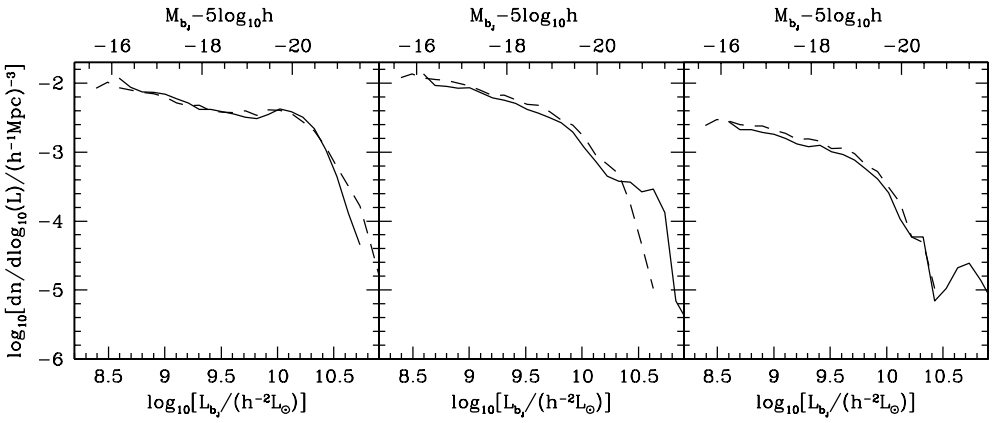

Figure 5. Galaxy $b_{\rm J}$ luminosity functions in haloes of different mass predicted by two semi-analytical models of galaxy formation. The panels refer to haloes with masses of $10^{x}\,h^{-1}\ {\rm M}_{\odot}$, with $x = 13 \pm 0.5$ (left), 14 ± 0.5 (centre) and 15 ± 0.5 (right). The scales at the top of the panels give the absolute $b_{\rm J}$ magnitude. Solid lines correspond to the 'bumpy' semi-analytical model, whereas dashed lines correspond to the 'superwind' model. Note that the lines for the superwind model in the larger groups terminate where there are no longer any bright galaxies.

Downloaded from https://academic.oup.com/mnras/article-abstract/355/3/769/952880 by California Institute of Technology user on 19 May 2020

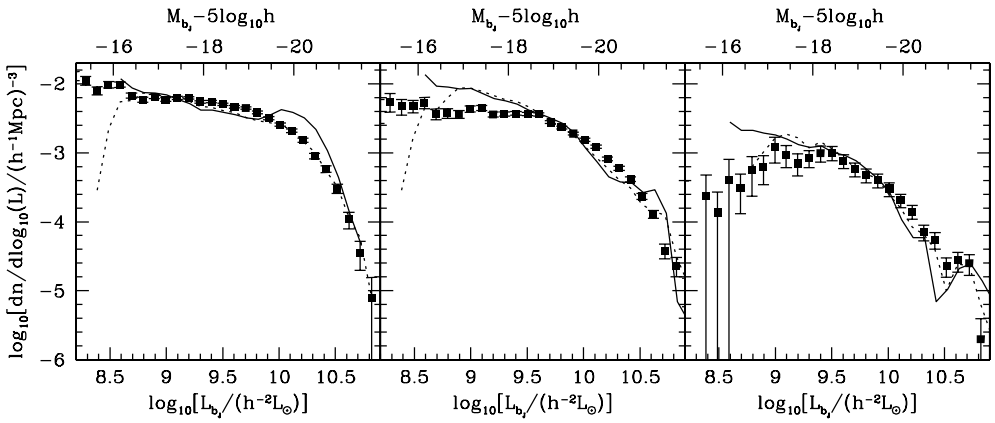

Figure 6. Galaxy b_J luminosity functions in groups of different mass in both mock and real 2PIGG catalogues. The group mass ranges are $M \sim 10^{13}\,h^{-1}$ $M_\odot$ (left), $M \sim 10^{14}\,h^{-1}$ $M_\odot$ (centre) and $M \sim 10^{15}\,h^{-1}$ $M_\odot$ (right). In each case, a solid line shows the semi-analytical prediction from which the mock catalogues were constructed, a dotted line shows what is actually measured in the mock groups, and the filled squares with errors depict the results from the 2PIGG data. The values of $n_{\rm min}$ and $z_{\rm max}$ are selected for each mass range, as described in the text, in order to optimize the recovery of the original galaxy semi-analytical luminosity functions.

respects, the real 2PIGG results look very similar to those recovered from the mock catalogue, shown as dotted lines. The main difference is the abundance of low-luminosity ($L < L_*/3$) galaxies in higher-mass haloes. The mock groups contain more of these galaxies than are present in high-mass 2PIGGs. This difference is apparent in the panels showing the $M \sim 10^{14}$ and $\sim 10^{15}\,h^{-1}$ $M_\odot$ results. The evidence for bumps in the 2PIGG data is also only tentative. Note that, the apparent deficit of galaxies with $\log_{10}[L_{b_J}/(h^{-2}\,L_\odot)] < 9$ in the biggest 2PIGGs is a result of the lack of nearby massive clusters, combined with the flux limit of the 2dFGRS. Consequently, this set of clusters would require deeper observations in order to provide any interesting information concerning the behaviour of the cluster galaxy luminosity function at these low luminosities.

Fig. 7 shows the 1, 2 and 3σ contours in the L_*–α plane for the Sandage, Tammann & Yahil (1979, hereafter STY) fits to the 2PIGG galaxy luminosity functions within groups of different mass. Also shown (without a symbol marking the most likely value) are the contours representing the best-fitting parameters for the whole galaxy population out to $z = 0.12$. The parameters for the highest-mass bin are much less well constrained because there are fewer total galaxies in these groups than in the more abundant, lower-mass haloes. The 2PIGG sample has a slightly brighter L_* for the $M \sim 10^{14}\,h^{-1}$ $M_\odot$ groups than the $M \sim 10^{13}\,h^{-1}$ $M_\odot$ groups. This trend is reproduced in the bumpy mock catalogue but not in the superwind mock, in which the most luminous galaxies no longer reside in the most massive haloes. Note that, for the more massive groups, a Schechter function becomes an increasingly bad fit to the data, so this figure should be treated with caution. The fact that the most likely cluster Schechter function parameters almost coincide with those of all $z < 0.12$ galaxies is little more than chance.

Fig. 8 shows how the recovered luminosity functions differ from the suitably normalized best-fitting Schechter functions for the 2PIGGs. While the fit works well for both mock and real data in the $M \sim 10^{13}\,h^{-1}$ $M_\odot$ groups, it becomes an increasingly poor description in more massive systems, where an excess of luminous galaxies can be seen to distort the fit. Also apparent is the overabundance of low-luminosity galaxies in the most massive mock groups relative to what is found in the 2PIGGs. Finally, the lack of very luminous galaxies in the superwind mock shows that, despite the imperfections of the recovery, it is still possible to discriminate between this and the bumpy model.

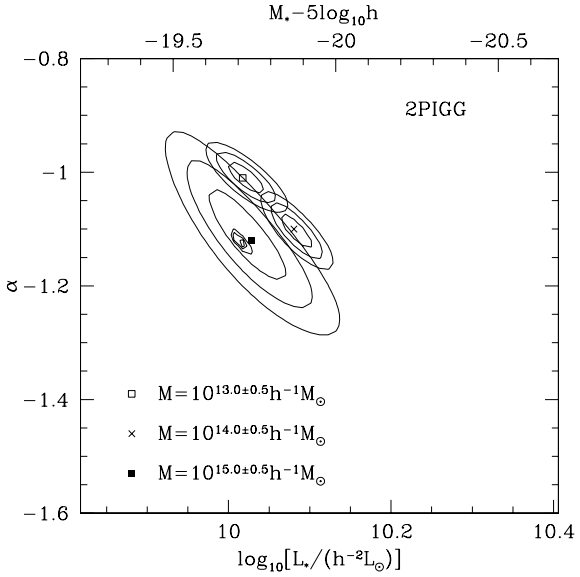

Figure 7. 1, 2 and 3σ contours showing the relative probability that different Schechter function parameters, L_* and α, provide a good description of the b_J-band galaxy luminosity function within 2PIGGs of different mass. These results were obtained by the STY estimation method using the groups contributing to the 2PIGG luminosity functions in Fig. 6. The different group masses have different symbols marking the most likely parameter values, as detailed in the figure. The small ellipses with no central symbol represent the results for all 2dFGRS galaxies at $z < 0.12$.

3.2 r_F-band results

The same analysis performed in Section 3.1 for the b_J-band data can be performed for the r_F-band data. While all galaxies can be used to calculate the luminosity functions using the $1/V_{\rm max}$ method, the STY estimation of the best-fitting Schechter function parameters requires a complete sample, so galaxies are only included if $14 < r_F < b_{J,\rm lim} - 1.5$ when determining L_* and α.

Figs 9–12 are the r_F-band equivalents of the previous four figures for the b_J band. Apart from larger error ellipses on the recovered Schechter function fits, resulting from the smaller number of galaxies being used to ensure a complete sample, the r_F-band results are

Downloaded from https://academic.oup.com/mnras/article-abstract/355/3/769/952880 by California Institute of Technology user on 19 May 2020

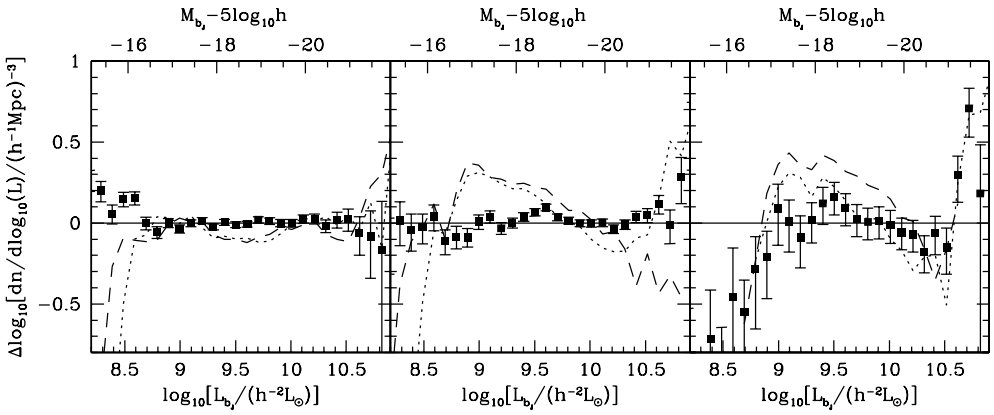

Figure 8. The ratios of galaxy luminosity functions to the 2PIGG best-fitting Schechter functions for the $M \sim 10^{13}\,h^{-1}\,\mathrm{M}_\odot$ (left), $M \sim 10^{14}\,h^{-1}\,\mathrm{M}_\odot$ (centre) and $M \sim 10^{15}\,h^{-1}\,\mathrm{M}_\odot$ (right) groups. Results are shown for 2PIGG (squares), the bumpy mock (dotted lines) and the superwind mock (dashed lines).

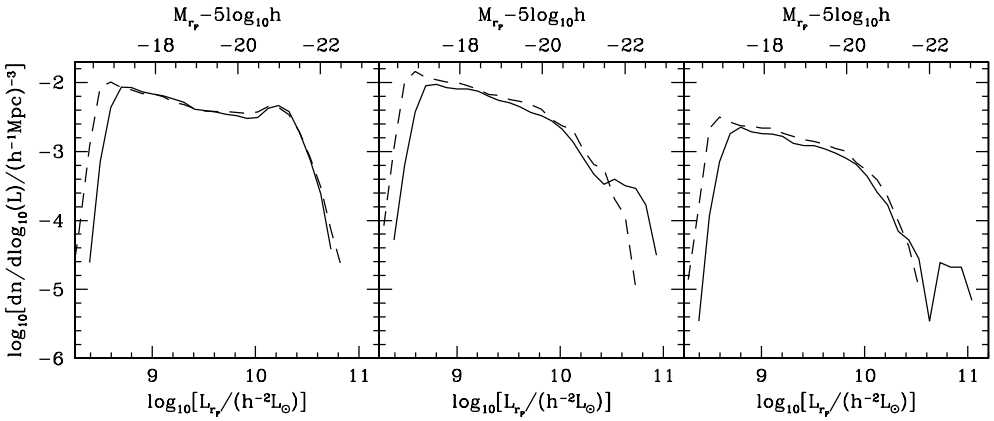

Figure 9. The r_F-band equivalent of Fig. 5, showing the galaxy luminosity functions in groups of different mass in the two semi-analytical models of galaxy formation. As before, the panels correspond to groups with $M = 10^{13\pm0.5}\,h^{-1}\,\mathrm{M}_\odot$ (left), $M = 10^{14\pm0.5}\,h^{-1}\,\mathrm{M}_\odot$ (centre) and $M = 10^{15\pm0.5}\,h^{-1}\,\mathrm{M}_\odot$ (right). Solid lines correspond to the 'bumpy' semi-analytical model, whereas dashed lines correspond to the 'superwind' model.

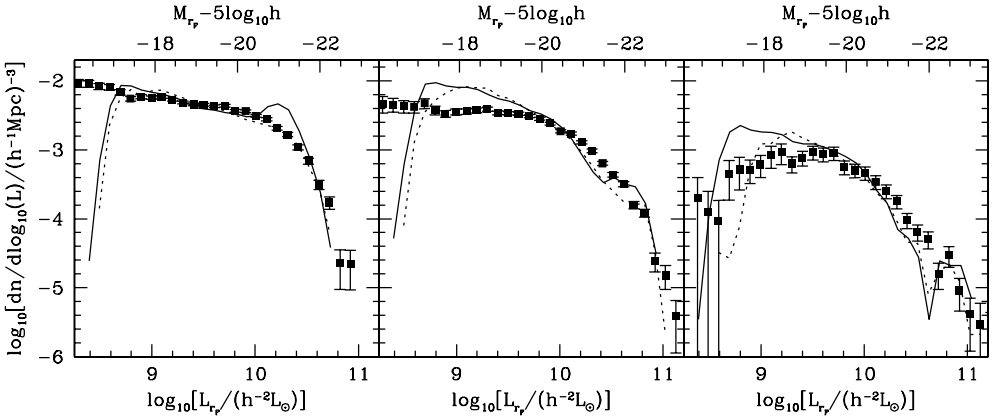

Figure 10. The r_F-band equivalent of Fig. 6 showing both how well the galaxy luminosity functions can be recovered in different sized groups, and how the mock results compare with the real 2PIGG data. As before, the group mass ranges are $M \sim 10^{13}\,h^{-1}\,\mathrm{M}_\odot$ (left), $M \sim 10^{14}\,h^{-1}\,\mathrm{M}_\odot$ (centre) and $M \sim 10^{15}\,h^{-1}\,\mathrm{M}_\odot$ (right). In each case, a solid line shows the semi-analytical prediction from which the mock catalogues were constructed, a dotted line shows what is actually measured in the mock groups, and the filled squares with errors depict the results from the 2PIGG data.

qualitatively very similar to those found in the b_J band. The 2PIGGs with $M \sim 10^{14}\,h^{-1}\,\mathrm{M}_\odot$ again have an average galaxy luminosity function with L_* approximately 25 per cent higher than that for the $M \sim 10^{13}\,h^{-1}\,\mathrm{M}_\odot$ groups, and a slightly steeper faint end slope. The bumpy mock reproduces this scaling of L_* with halo mass, but again contains an excess of low-luminosity galaxies in the most massive haloes. Once more, the superwind mock exhibits both an excess of low-luminosity galaxies and a deficit of high-luminosity

Downloaded from https://academic.oup.com/mnras/article-abstract/355/3/769/952880 by California Institute of Technology user on 19 May 2020

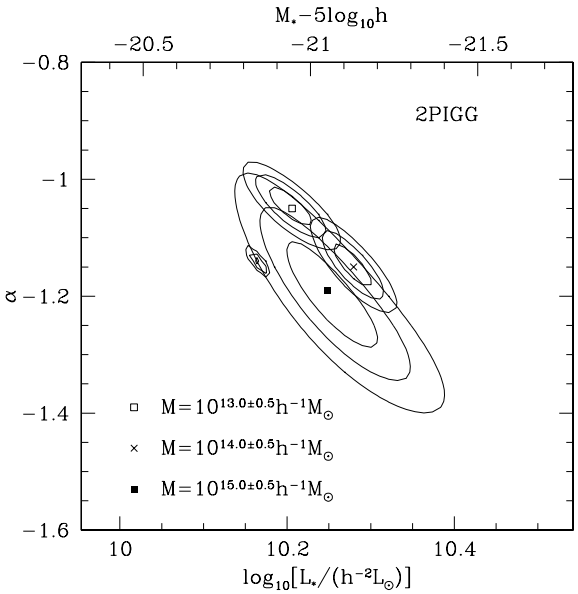

Figure 11. The r_F-band equivalent of Fig. 7, showing the STY-determined most likely Schechter function parameters for 2PIGG galaxy luminosity functions. The different group masses are represented by the contours enclosing the open square ($M = 10^{13\pm0.5}\,h^{-1}\,M_\odot$), cross ($M = 10^{14\pm0.5}\,h^{-1}\,M_\odot$) and filled square ($M = 10^{15\pm0.5}\,h^{-1}\,M_\odot$). Results for all galaxies satisfying $14 < r_F < b_{J,lim} - 1.5$ and $z < 0.12$ are shown by contours with no central symbol.

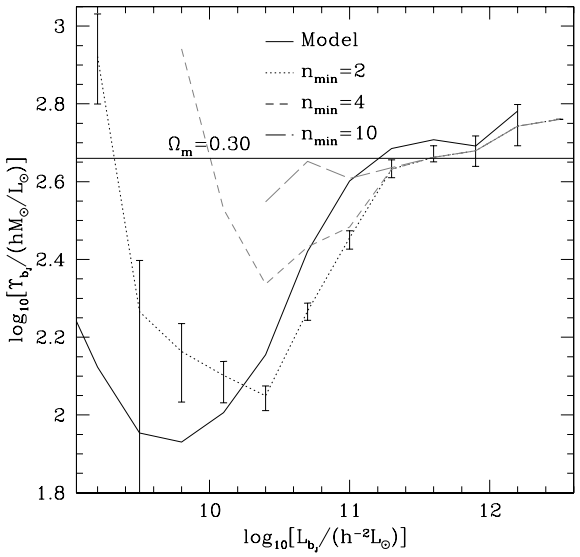

Figure 13. The group mass-to-light ratios as a function of group luminosity. The solid line traces the variation of the median Υ_{b_J} in the semi-analytical model from which the mock group catalogues were constructed. The dotted line shows the Υ_{b_J} actually recovered from the mock catalogue using groups with $n_{min} = 2$ that lie within a redshift of $z_{max} = 0.07 + 0.02\,[\log_{10}(L_{b_J}/h^{-2}\,L_\odot) - 10]$ and have no neighbouring groups with centres at distances less than $d_{min}/h^{-1}\,Mpc = 2 + [10 - \log_{10}(L_{b_J}/h^{-2}\,L_\odot)]$. Error bars represent the 16th and 84th percentiles divided by the square root of the number of groups contributing to each bin. This would be the standard deviation on the median if the Υ_{b_J} values were distributed normally in each bin. The corresponding measurements for the $n_{min} = 4$ and $n_{min} = 10$ samples are shown by the short- and long-dashed lines, respectively. The horizontal line indicates the mean mass-to-light ratio of the mock universe, calculated using the luminosity function of Norberg et al. (2002), and the appropriate value of $\Omega_m = 0.3$.

galaxies in both of the higher-mass bins, relative to the 2PIGG sample.

4 GROUP MASS-TO-LIGHT RATIOS

As outlined in Section 1, the mass-to-light ratio of groups, Υ, contains clues to the nature of galaxy formation, and it can also be used to estimate the mean mass density of the Universe. This section contains a description of the accuracy with which Υ can be determined from the 2PIGG catalogue, and addresses the dependence of Υ on group luminosity, the size of halo in which stars form most efficiently and the estimate of the mean mass density, Ω_m.

As discussed by Benson et al. (2000), the variation of group mass-to-light ratio with group size essentially reflects the efficiency of galaxy formation in different environments. The model predictions for this behaviour, shown in Figs 13–16, exhibit a minimum mass-to-light ratio for Local Group-sized haloes. In larger systems, cooling becomes increasingly less efficient, leaving a higher fraction of the group baryons outside of the member galaxies. For the smaller groups, it is feedback that suppresses the conversion of gas to stars, thus leading to the larger mass-to-light ratios seen in the figures.

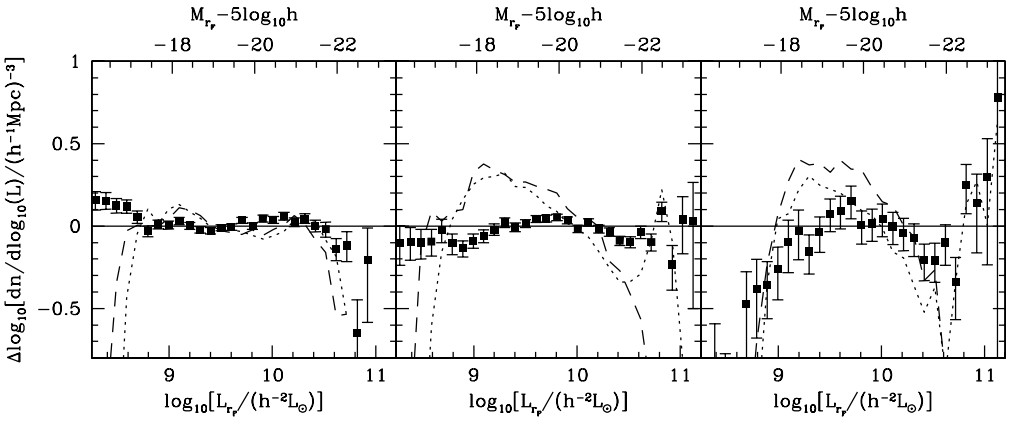

Figure 12. The r_F-band equivalent of Fig. 8, showing the ratios of galaxy luminosity functions in the 2PIGG (squares), bumpy mock groups (dotted lines) and superwind mock groups (dashed lines) to the best-fitting Schechter function for the 2PIGGs in each mass range. The mass ranges are: $M \sim 10^{13}\,h^{-1}\,M_\odot$ (left), $M \sim 10^{14}\,h^{-1}\,M_\odot$ (centre) and $M \sim 10^{15}\,h^{-1}\,M_\odot$ (right).

Downloaded from https://academic.oup.com/mnras/article-abstract/355/3/769/952880 by California Institute of Technology user on 19 May 2020

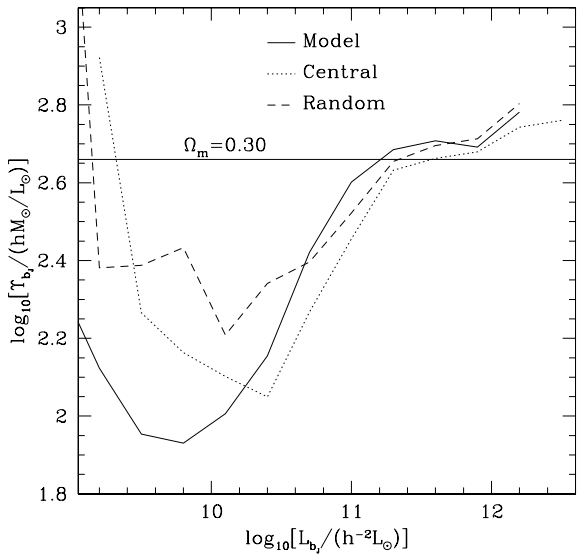

Figure 14. The effect of the positioning of the 'central' galaxy on the group mass-to-light ratio as a function of group luminosity. The solid and dotted lines show the same quantities as in the previous figure. A dashed line traces the $n_{\rm min} = 2$ results recovered from mock groups where the 'central' galaxy is placed at the position and velocity of a random dark matter group particle.

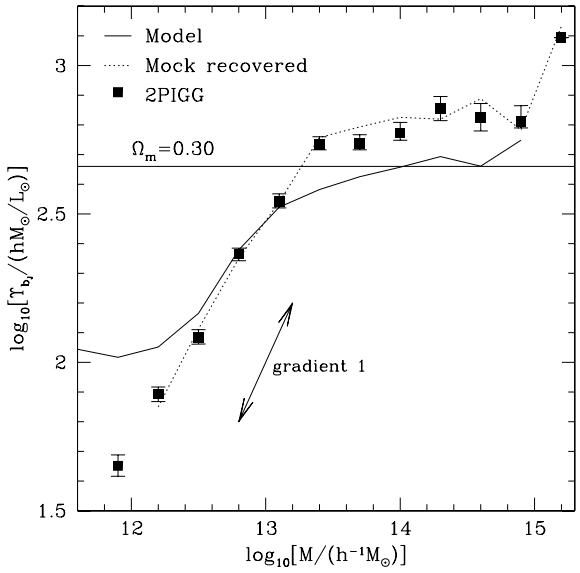

Figure 15. The group mass-to-light ratios as a function of group mass. The solid line traces the variation of the median Υ_{b_J} in the semi-analytical model from which the mock group catalogues were constructed. The dotted line shows the Υ_{b_J} actually recovered from the mock catalogue using groups with $n_{\rm min} = 2$ that lie within a redshift of $z_{\rm max} = 0.07 + 0.02\,[\log_{10}(L_{b_J}/h^{-2}\,{\rm L}_\odot) - 10]$ and have no neighbouring groups with centres at distances less than $d_{\rm min}/h^{-1}$ Mpc $= 2 + [10 - \log_{10}(L_{b_J}/h^{-2}\,{\rm L}_\odot)]$. The corresponding measurement from the 2PIGG sample is shown by the filled squares, with error bars representing the 16th and 84th percentiles divided by the square root of the number of groups contributing to each bin. A line with gradient 1 is also plotted to illustrate the direction in which errors in the inferred group masses would move the estimated values.

In trying to recover the typical group mass-to-light ratio for groups of a particular size, there is no reason to use the entire group sample. One merely requires an unbiased subset of groups. Experimentation with the mock catalogues has yielded an appropriate subset,

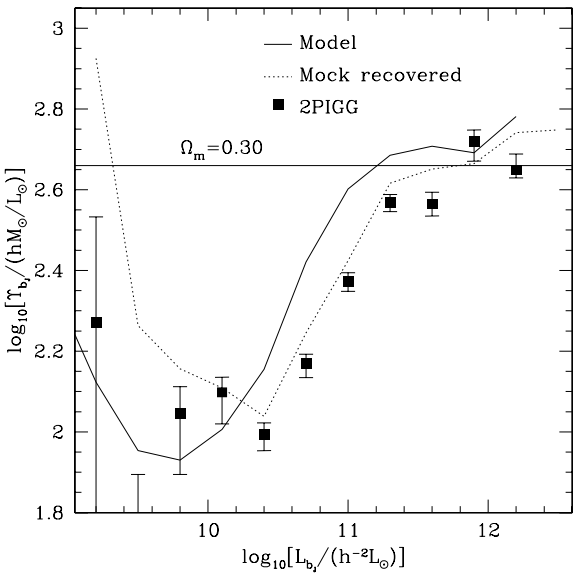

Figure 16. The median mass-to-light ratio of groups as a function of group luminosity. Line types and symbols are the same as in the previous figure, as are the values of $n_{\rm min}$, $z_{\rm max}$ and $d_{\rm min}$ defining the recovered groups.

in which the bias of the results is minimized. In this scheme, the smaller groups are only used when they are relatively nearby and isolated, whereas the restrictions are less stringent for larger groups. Specifically, of the $n_{\rm min} = 2$ groups, only those with $z < z_{\rm max} = 0.07 + 0.02[\log_{10}(L_{b_J}/h^{-2}\,{\rm L}_\odot) - 10]$ and having no neighbouring groups with centres at distances less than $d_{\rm min}/h^{-1}$ Mpc $= 2 + [10 - \log_{10}(L_{b_J}/h^{-2}\,{\rm L}_\odot)]$ were used to calculate the mass-to-light ratios. The reasons for the success of this empirical choice are as follows. Many of the small groups are fragments cleaved from much bigger groups by the group-finding algorithm. These typically have large velocity dispersions, reflecting the size of the halo to which they really belong. Consequently, their mass-to-light ratios are unrepresentatively high. The nearest-neighbour distance restriction is intended to eliminate these spurious groups from the analysis. The reason for the redshift limit is the desire that most underlying groups of a particular size should contain at least two galaxies that will be detected in a flux-limited survey. The mock catalogues used here are such that the true mass-to-light ratio of low-luminosity groups is typically lower for groups containing only one detectable galaxy. Thus, in order to ensure that the low-luminosity groups are representative of the underlying distribution, only the nearby low-luminosity examples are included.

Fig. 13 shows how the median mass-to-light ratio varies with group luminosity for the model groups, and how well it can be recovered from the mock catalogues. The luminosity bins with $9.7 < \log_{10}[L_{b_J}/(h^{-2}\,{\rm L}_\odot)] < 11.1$ all contain well over 200 groups. The size of the 2PIGG catalogue is thus sufficient to provide small statistical errors despite the large uncertainties associated with the individual mass measurements for groups containing only two galaxies (see Fig. 3). As the minimum number of galaxies per group is decreased, the recovered results trace the input model to smaller group luminosities. For instance, at $\log_{10}[L_{b_J}/(h^{-2}\,{\rm L}_\odot)] = 10.4$, where there are groups with as many as 10 galaxies, the least biased results are returned when all groups down to binaries are included. This occurs because the bulk of groups at this luminosity should only contain two or three galaxies. Those containing 10 galaxies are more likely to be projections of smaller systems that happen to lie along

Downloaded from https://academic.oup.com/mnras/article-abstract/355/3/769/952880 by California Institute of Technology user on 19 May 2020

a particular line of sight and will consequently have overestimated velocity dispersions, and therefore masses. Thus, from the point of view of systematic errors arising from the group-finding procedure, it is clear that using all groups down to the binaries produces a better recovery of the underlying model than restricting the sample to the more populated groups.

With the smaller groups, there is an additional concern that the positioning of galaxies within haloes in the model may not be similar to that in the real groups. For instance, the model assumes that one galaxy in every group is positioned at the mean position and velocity of the halo. In estimating the rms velocity dispersions and projected sizes, an extra factor of $\sqrt{n_{\rm gal}/(n_{\rm gal}-1)}$ is included to correct for the fact that one group member is not sampling the depth or size of the group potential. If, in real groups, all galaxies are placed randomly throughout the group potential, then this extra factor will be applied unnecessarily, leading to overestimates of the cluster mass. These will be larger for groups with smaller memberships. This is illustrated in Fig. 14, where the results of mock catalogues employing either a central or randomly placed 'central' group galaxy are shown. The impact of the systematic error in the mass estimation amounts to a shift of $\sim$0.2 in $\log_{10}\Upsilon_{b_{\rm J}}$ at $\log_{10}[L_{b_{\rm J}}/(h^{-2}\,{\rm L}_{\odot})]\approx 10$. This provides an upper limit to this particular systematic uncertainty, because some of the real groups will effectively have the 'central' galaxy at the halo centre. Note that any trend of decreasing mass-to-light ratio with decreasing group luminosity would be lessened by the inappropriate use of this correction. Thus, any such trend that is detected should only become stronger if this systematic error is important. In subsequent sections, it will be shown that the 2PIGG results exhibit a very similar trend of mass-to-light ratio with group luminosity to those from the mock catalogues. This suggests that no gross systematic differences exist between the mock groups and the 2PIGGs.

A further check of systematic errors can be made by splitting the groups into two samples based on whether they are at redshifts above or below the median value for groups contributing to each luminosity bin. This exercise has been performed and confirms that no significant redshift-dependent systematic effect is evident across the full range of group sizes probed here.

The mass-to-light ratio of the majority of the model groups is significantly lower than the universal mean, reflecting the relatively high efficiency of galaxy formation in these haloes. While such groups contain many of the galaxies in the survey, the model places a large fraction of the mass in low-luminosity haloes that are off the left-hand side of these figures.

The following two subsections describe the $b_{\rm J}$- and $r_{\rm F}$-band results. The redder band traces the stellar mass more faithfully than the blue band, and $\Upsilon_{r_{\rm F}}$ thus provides additional useful information.

4.1 $b_{\rm J}$-band results

Fig. 15 shows the dependence of $\Upsilon_{b_{\rm J}}$ on group mass in the model and in the 2PIGG sample. The horizontal line indicates the mean mass-to-light ratio in the mock universe, and the other solid line represents the variation of the median group $\Upsilon_{b_{\rm J}}$ with halo mass in the simulation with semi-analytical model galaxies from which the mock catalogues were constructed. A dotted line traces what is actually recovered from the mock catalogue, and the filled squares show the results from the real 2PIGG subsample of groups. Error bars represent the 16th and 84th percentiles divided by the square root of the number of groups in each bin. As a result of the large spread of accuracies in the inferred group masses for groups containing only a few members, there is a strong smearing effect along a line of gradient one. For the highest-mass groups, for which more galaxies yield better mass estimates, this trend is reduced, but there is sufficient contamination from low-luminosity groups with greatly overestimated masses, that the recovered $\Upsilon_{b_{\rm J}}$ is still biased high by 30–40 per cent. The main reason why the mock recovered variation resembles the true behaviour in the parent simulation at intermediate masses is that this is where the majority of the groups are found (see Fig. 1), so there are comparable numbers of groups biasing the results high and low. In summary, this figure demonstrates that it is unhelpful to plot correlated variables when they both suffer from the same large uncertainty.

A much better method for ordering groups in terms of size is to use their measured luminosities; these have much smaller errors than the group masses, particularly for groups with only two members (see Fig. 3). Now, instead of mass errors smearing out the results along a line of gradient one, there are luminosity uncertainties that act along a line of gradient -1. The sign of this gradient is opposite to the trend of $\Upsilon_{b_{\rm J}}$ with halo luminosity in the parent simulation, and the amplitude of this error vector is now substantially reduced. Fig. 16 shows the corresponding variation of group mass-to-light ratio with group luminosity.

In the semi-analytical model, the variation of $\Upsilon_{b_{\rm J}}$ reflects the efficiency of star formation in haloes of different mass. Star formation is most efficient in haloes with $L\approx 6\times 10^{9}\,h^{-2}\ {\rm L}_{\odot}$, the point at which the minimum of the solid line occurs. The dotted line traces the variation of $\Upsilon_{b_{\rm J}}$ recovered from the group mock catalogue. It is immediately apparent that this recovery, for haloes with $L_{b_{\rm J}}\gtrsim 10^{10}\,h^{-2}\,{\rm L}_{\odot}$, is very much better than was the case when group mass was used to quantify halo size. In particular, both the rise in $\Upsilon_{b_{\rm J}}$ from small groups to clusters, and the plateau for the largest clusters are well reproduced. There is a slight bias low, by $\sim$40 per cent, during the rise. This can be understood in terms of the position of the peak in the distribution of groups as a function of luminosity (Fig. 2), and the typical errors being made, whereby luminosities are slightly overestimated as a result of contamination (Fig. 4). The recovery of the mass-to-light ratio for groups less luminous than L_{*} (for galaxies) is poor. Among the reasons for this is the fact that the individual redshift measurement errors become comparable with the typical group velocity dispersions in such small systems. Also, there is insufficient volume to achieve small statistical errors while ensuring that these groups contain more than one detectable galaxy.

One way to estimate the mean mass density of the real Universe is to measure the mass-to-light ratio of the largest clusters, assume that it is typical of the Universe as a whole, and then use this factor to convert the measurable mean light density of the Universe into an estimate of $\Omega_{\rm m}$. As Fig. 16 shows that the mass-to-light ratio of objects depends upon the total group luminosity, the definition of a 'large cluster' is one that should pick only those systems that lie at high luminosities where there is a plateau in the mass-to-light ratio. In the model, mock recovered and 2PIGG cases, a minimum group luminosity of $\log_{10}[L_{b_{\rm J}}/(h^{-2}\,{\rm L}_{\odot})]=11.5$ serves for this purpose, while ensuring that enough clusters are available for analysis. For the 111 groups with $\log_{10}[L_{b_{\rm J}}/(h^{-2}\,{\rm L}_{\odot})]>11.5$ in the mock catalogue, the recovered median and mean mass-to-light ratios are 471 and $549\pm 28\,h\ {\rm M}_{\odot}/{\rm L}_{\odot}$, respectively. The corresponding values in the parent simulation are 507 (median) and 520 (mean). Thus, the mean is overestimated in the mock values by $\sim$6 per cent, while the recovered median is 7 per cent too low. As the mean is more easily affected by outlying data points with high measurement errors, in what follows only the median cluster mass-to-light ratio will be used. The estimate of $\Omega_{\rm m}$ from the cluster mass-to-light ratio is based on comparing this to the mean mass-to-light ratio of the Universe. In

Downloaded from https://academic.oup.com/mnras/article-abstract/355/3/769/952880 by California Institute of Technology user on 19 May 2020

the parent simulation, the mean universal value is $458\,h\,\mathrm{M}_\odot/\mathrm{L}_\odot$, 10 per cent lower than the median recovered mass-to-light ratio of clusters. Thus, for this mock catalogue at least, the median mass-to-light ratio of the recovered clusters allows a reasonably accurate estimate of the mean mass density of the simulated universe.

The filled squares with error bars in Fig. 16 represent the real 2PIGG mass-to-light results. These are remarkably similar to what was recovered from the mock catalogue, showing the same three basic features: nothing useful at $L \lesssim 10^{10}\,h^{-2}\,\mathrm{L}_\odot$, a rise by a factor of $\sim$5 up to $L \sim 2 \times 10^{11}\,h^{-2}\,\mathrm{L}_\odot$, and a constant mass-to-light ratio for the largest groups. Unlike the case when mass was used to quantify the group size, this trend of increasing median mass-to-light ratio with larger groups can no longer be confused with the effect of mass measurement errors. For the $\log_{10}[L_{b_\mathrm{J}}/(h^{-2}\,\mathrm{L}_\odot)] > 11.5$ groups, of which there are 96, the median $\Upsilon_{b_\mathrm{J}} = 429 \pm 25\,h\,\mathrm{M}_\odot/\mathrm{L}_\odot$, where the uncertainty represents the statistical error on the median. This number is used later to estimate Ω_m.

4.2 Comparison with other studies

When comparing these results with other studies, it is essential to bear in mind that there exists a variety of definitions of a group. To reiterate, the 2PIGG analysis is designed to recover, as well as possible, groups that resemble those identified in a ΛCDM dark matter simulation using the standard linking length of 0.2 times the mean interparticle separation. Note that in Fig. 17, the raw 2PIGG results are shown for the purpose of comparison with other studies, despite the fact that they probably suffer from a small bias of the sort shown in Fig. 16. In Section 4.4, this bias is corrected and functions are given that describe the variation of the corrected median group mass-to-light ratio with group luminosity.

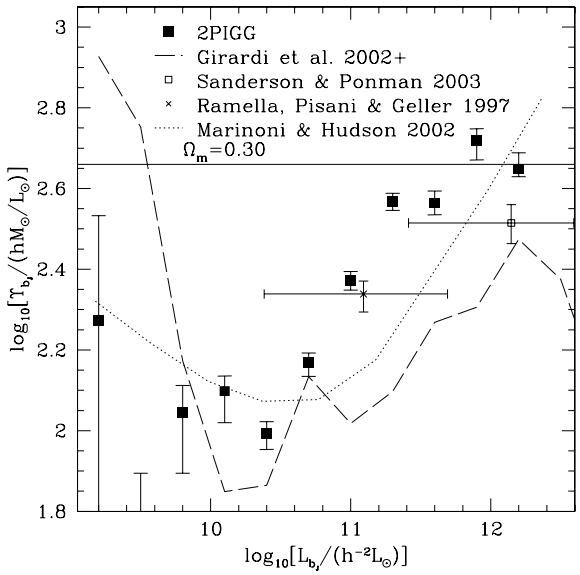

Figure 17. The median mass-to-light ratio of groups as a function of group luminosity. As in the previous figure, filled squares represent results for the 2PIGG sample. The horizontal line indicates the mean mass-to-light ratio determined from the mean luminosity density of Norberg et al. (2002), assuming $\Omega_\mathrm{m} = 0.3$. The results of four other studies of B-band group mass-to-light ratios are also shown, as indicated in the legend. Vertical error bars on the data points give the uncertainty on the median Υ_{b_J}. The horizontal error bars represent the 16–84th percentile range of the group luminosities contributing to these medians.

The results of Girardi et al. (2002, G2002), which extend the data base used by Girardi et al. (2000) with groups mostly found in the Nearby Optical Galaxy (NOG) catalogue, contain groups from a number of different surveys. Note that these papers both contain a typographical error relating to the conversion between B and b_J magnitudes (Girardi, private communication). The correct relation, for a mean galaxy colour of $(B - V) = 0.9$, is

$$B - b_\mathrm{J} = 0.252. \tag{4.1}$$

In conjunction with

$$(B - b_\mathrm{J})_\odot = 0.15, \tag{4.2}$$

this leads to

$$\frac{\left(L/\mathrm{L}_\odot\right)_{b_\mathrm{J}}}{\left(L/\mathrm{L}_\odot\right)_B} = 1.1, \tag{4.3}$$

as was correctly reported in G2002. Fig. 17 shows the data from the (CL+PS) sample of G2002, supplemented with 500 other systems from their set of groups found by applying a percolation algorithm to the NOG survey (Girardi, private communication). Relative to the homogenous 2PIGG sample, this set of groups comes from a number of different sources and, furthermore, they were analysed using different types of mass and luminosity estimators. Yet, a broadly similar behaviour of the mass-to-light ratio is seen. Care is needed, however, because the percolation algorithm of G2002 will presumably yield results that are biased to low mass-to-light ratios, for the same reason that the 2PIGG results are affected. Their percolation algorithm (Giuricin et al. 2000) employs a scaling of the linking volume with redshift that is different from that used for the 2PIGG catalogue (Eke et al. 2004), so the properties of the recovered groups will be different.

Sanderson & Ponman (2003) used a sample of 32 systems with masses inferred from their X-ray emission. These groups are concentrated towards the large-mass end of the distribution and show little or no trend of mass-to-light ratio with group luminosity, comparable with the 2PIGG results. Again, their results yield slightly lower values of the mass-to-light ratio than are found for 2PIGG. Note that the point plotted in the figure differs very slightly from that in the Sanderson & Ponman paper as a result of the correction of an error in their B to b_J conversion for three groups.

Ramella et al. (1997) used a sample of 406 groups identified in the northern CfA2 survey, with masses estimated from optical data. While the median mass-to-light ratio is lower than that of the Sanderson & Ponman groups, the CfA2 groups are typically smaller and the 2PIGG results indicate that Υ_{b_J} should be smaller for such groups. However, once more, the mass-to-light ratio in this sample is lower than that inferred from the 2PIGG catalogue.

Marinoni & Hudson (2002) have indirectly inferred a mass-to-light ratio variation for groups by finding the mapping between the Press & Schechter (1974) mass function, for some assumed cosmological model, and the luminosity function of groups measured from the NOG sample by Marinoni, Hudson & Giuricin (2002). Their results are given in the B band, and have been converted to the b_J band using equation (4.3). This curve shows a similar trend to the 2PIGG results but, again, with an offset. In general, estimators of the luminosity function of groups tend to be biased towards high luminosities as a result of the inevitable inclusion of interlopers in the groups, the statistical errors in the inferred group luminosities and the steep decline in the abundance of objects with increasing size. This would lead to an overestimate of the luminosity at a particular abundance (or mass), biasing low the inferred mass-to-light ratio. Indeed, estimating the luminosity function of groups in mock

Downloaded from https://academic.oup.com/mnras/article-abstract/355/3/769/952880 by California Institute of Technology user on 19 May 2020

2PIGG catalogues suggests that this bias could plausibly yield an overestimate of the group luminosity by a factor of at least 2 at a particular abundance (Eke et al. in preparation). If a similar size of bias were present in the sample used by Marinoni & Hudson, then this would account for their significantly lower mass-to-light ratios at $L \sim 10^{11}\,h^{-2}\ \mathrm{L}_{\odot}$.

One factor that would bias the 2PIGG mass-to-light values slightly high is the incompleteness in the parent 2dFGRS catalogue (Pimbblet et al. 2001; Norberg et al. 2002; Cross et al. 2004). This arises largely from incorrect image classification in the parent catalogue, and is roughly independent of galaxy magnitude. Ideally one would want to correct the 2PIGG luminosities for this effect but, as the effect is small (a ∼9 per cent loss of galaxies) and somewhat uncertain, such a correction has not been applied here. Relative to the difference between the 2PIGG and other results in Fig. 17, this factor is insignificant. The most likely other reason why the 2PIGG results could be systematically incorrect is if the mass estimator employed here is not appropriate in the real world, as discussed in Section 2. This would happen if galaxies traced real dark matter haloes in a different way from what was assumed in making the mock catalogues, either because they had a different velocity dispersion to the underlying dark matter, or because they had a different projected spatial distribution (De Lucia et al. 2004; Diemand, Moore & Stadel 2004). In order for biases of this kind to give rise to the observed variation of the mass-to-light ratio with group size, however, they would need to depend very strongly on group size. It is difficult to imagine that such biases could give rise to the factor of ∼5 variation seen in the data.

4.3 r_{F}-band results

As described in the Appendix, the 2dFGRS data combined with the SuperCOSMOS r_{F} data provide a well-defined sample of galaxies with $14 < r_{\mathrm{F}} < b_{\mathrm{J,lim}} - 1.5$. While applying these flux limits reduces the number of galaxies available to calculate the group luminosity, the missing faint galaxies contribute little to the total, so the accuracy with which group r_{F}-band luminosities can be inferred is comparable to that for the b_{J} band, as was shown in Section 2.2.

Fig. 18 shows how well the variation of $\Upsilon_{r_{\mathrm{F}}}$ in the parent simulation can be recovered in the mock catalogue, as a function of group b_{J} luminosity. (This is a slightly better determined measure of 2PIGG size than the r_{F} luminosity.) The results are remarkably similar to those shown in Fig. 16 for $\Upsilon_{b_{\mathrm{J}}}$. First, the intrinsic variation present in the parent simulation is quite accurately recovered in the mock catalogues. Secondly, as was the case for $\Upsilon_{b_{\mathrm{J}}}$, the 2PIGG data agree remarkably well with the behaviour seen in the mock catalogue. The main difference between the r_{F} and b_{J} results is the size of the change in typical mass-to-light ratio over the reliably probed range of group luminosities. This is not as extreme in the r_{F} band, a factor of ∼3.5 rather than the factor of ∼5 seen in the b_{J} band – as one would expect if halo size has a stronger effect on recent star formation than on the overall stellar mass.

Fig. 19 compares the 2PIGG results with those from CNOC groups and clusters (Carlberg et al. 1996, 2001) and the LCRS groups (Tucker et al. 2000). Unlike in the b_{J}-band case, there is now some agreement between the 2PIGGs and some other work. Note that the Carlberg et al. data points have luminosities measured in the Gunn *r* band and include a correction to redshift zero, whereas the Tucker et al. data are measured in the LCRS *R* band. Once again, the horizontal error bars illustrate the 16–84th percentile range in group luminosity contributing to each point.

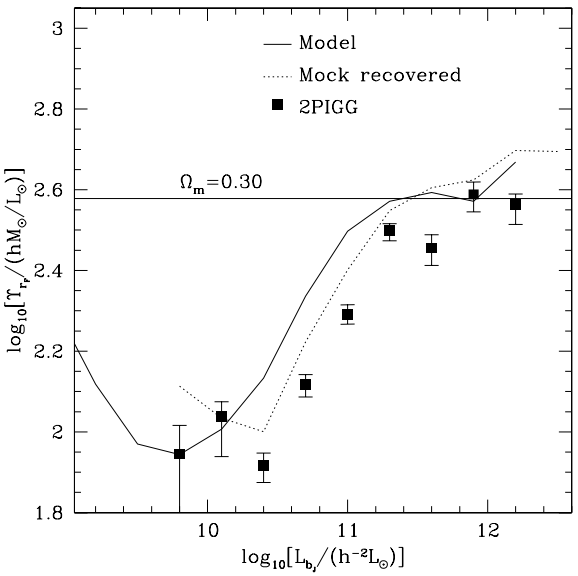

Figure 18. The variation of the r_{F}-band group mass-to-light ratio with group b_{J} luminosity. A solid line traces the median behaviour in the parent simulation, and the dotted line shows what is actually recovered in the mock catalogue. Filled squares represent the results from the 2PIGG catalogue, using the same redshift and minimum group separation as were applied to the b_{J}-band data.

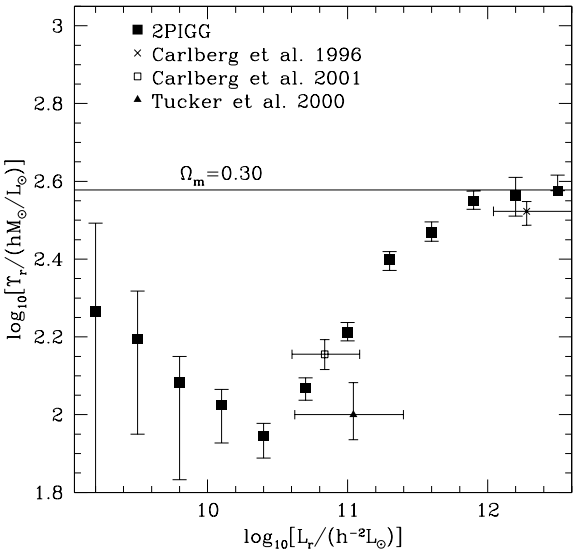

Figure 19. The variation of the *R*-band group mass-to-light ratio with group luminosity. Filled squares represent the results from the 2PIGG catalogue, and the other symbols show other observational determinations, as detailed in the legend. Note that the Carlberg et al. results have luminosities measured in the Gunn *r* band, and the Tucker et al. data are in the LCRS *R* band.

4.4 Corrected mass-to-light results

It was shown in Sections 4.1 and 4.3 that the values of Υ as a function of $L_{b_{\mathrm{J}}}$ recovered in the mock catalogues are slightly biased low relative to the values in the parent simulation. This bias is reproducible in mock catalogues constructed from other simulations, for example, from the less clustered mass distribution of a ΛCDM

Downloaded from https://academic.oup.com/mnras/article-abstract/355/3/769/952880 by California Institute of Technology user on 19 May 2020

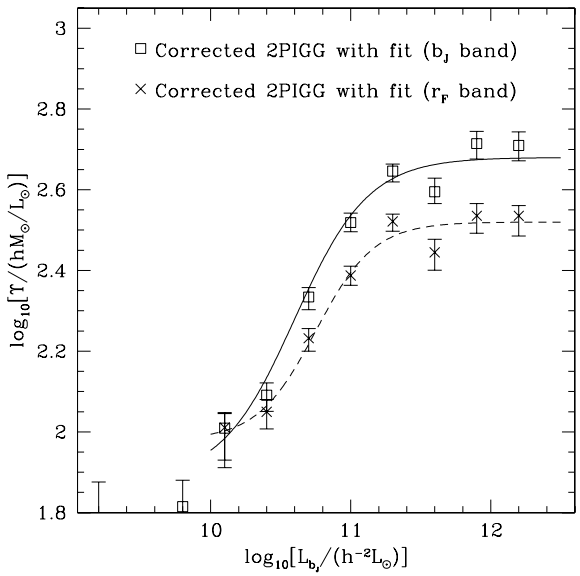

Figure 20. The corrected variation of the 2PIGG group mass-to-light ratio with group luminosity, in both the b_J and r_F bands. Equations (4.4) for Υ_{b_J} and (4.5) for Υ_{r_F} are shown as solid and dashed lines. The corresponding 2PIGG data are shown with open squares and crosses.

simulation with $\sigma_8 \approx 0.7$ analysed at $z \approx 0.1$ (rather than the default simulation with $\sigma_8 = 0.9$ and $z = 0.1$).

It seems plausible that a bias of this kind is also present in the 2PIGG sample results. A correction factor is defined as the ratio between the luminosity-dependent values of Υ measured in the parent simulation and in the mock catalogues (in both the b_J and r_F bands). The 2PIGG results are simply multiplied by this factor to obtain an estimate of the true underlying group mass-to-light ratio variation in the real Universe. The corrected values are shown with open squares (b_J band) and crosses (r_F band) in Fig. 20. The error bars on the data points still represent the size of the statistical uncertainty on the median. Approximate fits to the corrected 2PIGG median mass-to-light ratios are shown by the solid (b_J) and dashed (r_F) lines, which have the following functional forms:

$$\log_{10}\Upsilon_{b_J} = 2.28 + 0.4\tanh\{1.9\,[\log_{10}(L_{b_J}) - 10.6]\} \quad (4.4)$$

and

$$\log_{10}\Upsilon_{r_F} = 2.25 + 0.27\tanh\{2.4\,[\log_{10}(L_{b_J}) - 10.75]\}. \quad (4.5)$$

These equations are valid for $10 \leqslant \log_{10}(L_{b_J}/h^{-2}\,L_\odot) \leqslant 12.5$. As the 2PIGG results are so similar to those recovered from the mock catalogue, these fits to the underlying 'truth' in the real Universe also provide a decent description of the behaviour in the parent simulation, as traced by the solid lines in Figs 16 and 18. The correction is sufficiently small that all the basic features of the results discussed above remain.

The correction changes the median mass-to-light ratio of the 98 clusters with $\log_{10}[L_{b_J}/(h^{-2}\,L_\odot)] > 11.5$ from $\Upsilon_{b_J} = 427 \pm 24\,h\,M_\odot/L_\odot$ to $466 \pm 26\ h\ M_\odot/L_\odot$. Together with the global mean b_J-band luminosity density and its uncertainty, inferred from the luminosity function measured by Norberg et al. (2002), this implies [1] that $\Omega_m = 0.31 \pm 0.03$. If, as was the case in the mock catalogues, the median mass-to-light ratio of the largest clusters overestimates the mean mass-to-light ratio of the Universe by ∼11 per cent, then this estimate should come down accordingly to $\Omega_m = 0.28 \pm 0.03$ (statistical error only). While this correction factor is clearly model dependent, the fact that the global galaxy luminosity function and the bright end of the galaxy luminosity function in clusters are similar in both the mock catalogue and the 2PIGG data is suggestive that this is an appropriate thing to do. Any semi-analytical model yielding a mock catalogue that does not reproduce these observational constraints will probably provide a different correction factor that will very probably be inappropriate. The Ω_m estimate suffers from a number of systematic uncertainties, each of which is of a similar size to the overall statistical uncertainty. In addition to the two model-dependent corrections already applied (i.e. the bias introduced when measuring the mass-to-light ratio of the clusters and the difference between the cluster and mean Universal mass-to-light ratios), errors could arise from incorrect estimations of either cluster luminosities or masses. The former might come from incompleteness in the parent 2dFGRS catalogue. In fact, Norberg et al. (2002) do assume a 9 per cent incompleteness in the 2dFGRS parent catalogue when computing the mean b_J-band luminosity density of the Universe, so for consistency the 2PIGG luminosities should be similarly increased. The resulting lower mass-to-light ratios yield $\Omega_m = 0.26 \pm 0.03$ (statistical error only). Cluster masses will only be accurately inferred if the real galaxies populate haloes in the same way that mock galaxies do. This is likely to be the largest systematic uncertainty in the estimate of Ω_m and, as was discussed in Section 2, could amount to a fractional error of a few tens of per cent.

It is interesting that both this estimate of Ω_m and its statistical uncertainty are very similar to the values quoted by Spergel et al. (2003) from the combination of WMAP microwave background data and the 2dFGRS galaxy power spectrum. This agreement, in itself, suggests that the systematic uncertainties in either estimate are likely to be small and provides a welcome consistency check of the entire paradigm of structure formation by hierarchical clustering from CDM initial conditions. Further reassurance can be gained from using the r_F-band mass-to-light ratios of the same set of the most luminous clusters and the r_F-band luminosity density of the Universe (see the Appendix). This yields an estimate of $\Omega_m = 0.29 \pm 0.04$, which is consistent with the value inferred from the b_J-band data.

5 CONCLUSIONS

This paper presents an analysis of the galactic content of the 2PIGG catalogue of groups and clusters identified in the 2dFGRS, focusing on the galaxy luminosity function and total mass-to-light ratio in groups of different size in both the b_J and r_F bands. In constructing the 2PIGG catalogue (Eke et al. 2004) and in the present analysis, a well-defined methodology has been followed based on the extensive use of mock catalogues. The starting points are N-body simulations of the evolution of dark matter in a ΛCDM universe in which model galaxies are added with properties calculated according to a semi-analytical model of galaxy formation based on the precepts laid out in Cole et al. (2000). The parent simulation provides a full description of the model galaxy distribution, free from the distortions inevitably introduced by observational procedures, such as selection effects, observational errors, etc. These distortions are modelled carefully in order to generate mock catalogues that correspond to artificial 2dFGRSs. As the properties of the parent simulation are known, the mock catalogues provide a rigorous way to quantify the systematic uncertainties in the derived properties of interest and a good guide to possible systematic errors. Of course,

[1] Assuming that the galaxies trace the mass in clusters, as is customary when using this method

Downloaded from https://academic.oup.com/mnras/article-abstract/355/3/769/952880 by California Institute of Technology user on 19 May 2020

the mock catalogues also enable a detailed comparison between the real data and the model from which the mock catalogues were generated.

The main results of this paper are given as follows.

(i) The galaxy luminosity function is different in groups of different mass. These luminosity functions are moderately well described by Schechter functions for which, as the group mass increases, the characteristic luminosity, L_*, increases and the faint end slope, α, becomes more negative. However, the galaxy luminosity functions in the groups found in the original simulations are not well described by Schechter functions. For example, they exhibit a 'bump' at the bright end where the amplitude varies with group mass, reflecting the relative importance of the central galaxy and the satellites in the groups. Hints of bumps are also found in the largest 2PIGG clusters.

(ii) The median group mass-to-light ratio, Υ, also varies with halo size (which is most robustly characterized by total $b_{\rm J}$ halo luminosity). The mock catalogues indicate that, in the 2PIGG catalogue, Υ is reliably determined for groups of size ranging from that of the Local Group to the richest clusters in the survey. Over this range, which extends from $L_{b_{\rm J}} = 10^{10}$ to $10^{12}\,h^{-2}\,{\rm L}_\odot$, $\Upsilon_{b_{\rm J}}$ increases by a factor of 5, whereas $\Upsilon_{r_{\rm F}}$ increases by a factor of 3.5. At the highest luminosities, Υ becomes roughly constant in both bands. The semi-analytical models predict an upturn in Υ at luminosities lower than $L_{b_{\rm J}} \sim 10^{10}\,h^{-2}\,{\rm L}_\odot$ at which galaxy formation is most efficient. Unfortunately, the 2PIGG catalogue does not contain enough small groups with sufficiently accurate estimates of Υ to locate the theoretically expected minimum.

(iii) For the $L_{b_{\rm J}} > 3 \times 10^{11}\,h^{-2}\,{\rm L}_\odot$ objects, the median mass-to-light ratio is $\Upsilon_{b_{\rm J}} = 466 \pm 26$ (statistical) $h\,{\rm M}_\odot/{\rm L}_\odot$, independently of cluster size. Assuming that this value differs from the cosmic mean in the same small way that it does in the mock catalogue allows a determination of the mean cosmic density, $\Omega_{\rm m}$. Adopting the $b_{\rm J}$ luminosity density inferred from the 2dFGRS galaxy luminosity function by Norberg et al. (2002), leads to $\Omega_{\rm m} = 0.26 \pm 0.03$. (This estimate includes two small corrections derived from the mock catalogues as discussed in Section 4.4, and a third small correction for incompleteness in the 2dFGRS parent catalogue.) This value and its uncertainty are in excellent agreement with the values inferred by Spergel et al. (2003) from a combination of microwave background data and the galaxy power spectrum in the 2dFGRS.

The agreement of the 2PIGG results with the predictions of the simulations is impressive, and provides confidence in the basic picture of galaxy groups tracing virialized haloes of dark matter, even for those haloes that contain only a few observable galaxies. The simulations suggest two fruitful avenues for improving upon this work: (i) probe smaller groups to test whether the M/L ratio does indeed pass through the expected minimum around a group mass of $10^{12}\,h^{-1}\,{\rm M}_\odot$ and (ii) create catalogues with better resolved groups to see if the non-Schechter nature of the theoretically predicted luminosity functions can be revealed. Both of these targets will require new large redshift surveys that probe substantially further down the luminosity function than is possible with the current data set.

ACKNOWLEDGMENTS

The 2dF Galaxy Redshift Survey was made possible through the dedicated efforts of the staff of the Anglo-Australian Observatory, both in creating the 2dF instrument and in supporting its use on the telescope. VRE and CMB are Royal Society University Research Fellows. PN is a Zwicky Fellow. JAP and OL are PPARC Senior Research Fellows.

REFERENCES

Adami C., Mazure A., Biviano A., Katgert P., Rhee G., 1998, A&A, 331, 493
Balogh M. L., Christlein D., Zabludoff A. I., Zaritsky D., 2001, ApJ, 557, 117
Beers T. C., Flynn K., Gebhardt K., 1990, AJ, 100, 32
Benson A. J., Cole S., Frenk C. S., Baugh C. M., Lacey C. G., 2000, MNRAS, 311, 793
Benson A. J., Lacey C. G., Baugh C. M., Cole S., Frenk C. S., 2002, MNRAS, 333, 156
Benson A. J., Bower R. G., Frenk C. S., Lacey C. G., Baugh C. M., Cole S., 2003a, ApJ, 599, 38
Benson A. J., Frenk C. S., Baugh C. M., Cole S., Lacey C. G., 2003b, MNRAS, 343, 679
Blanton M. R. et al., 2001, AJ, 121, 2358
Blanton M. R. et al., 2003, ApJ, 592, 819
Bruzual G. A., Charlot S., 1993, ApJ, 405, 538
Carlberg R. G., Yee H. K. C., Ellingson E., Abraham R., Gravel P., Morris S., Pritchet C. J., 1996, ApJ, 462, 32
Carlberg R. G., Yee H. K. C., Morris S. L., Lin H., Hall P. B., Patton D. R., Sawicki M., Shepherd C. W., 2001, ApJ, 552, 427
Christlein D., 2000, ApJ, 545, 145
Christlein D., Zabludoff A. I., 2003, ApJ, 591, 764
Cirimele G., Nesci R., Trèvese D., 1997, ApJ, 475, 11
Cole S., Lacey C. G., Baugh C. M., Frenk C. S., 2000, MNRAS, 319, 168
Cole S. et al. (The 2dFGRS Team), 2001, MNRAS, 326, 255
Colless M. et al. (The 2dFGRS Team), 2001, MNRAS, 328, 1039
Colless M. et al. (The 2dFGRS Team), 2003, preprint (astro-ph/0306581)
Cross N. J. G., Driver S. P., Liske J., Lemon D. J., Peacock J. A., Cole S., Norberg P., Sutherland W. J., 2004, MNRAS, 349, 576
David L. P., Jones C., Forman W., 1995, ApJ, 445, 578
Davis M., Efstathiou G., Frenk C. S., White S. D. M., 1985, ApJ, 292, 371
De Lucia G. et al., 2004, MNRAS, 348, 333
de Propris R. et al. (The 2dFGRS Team), 2003, MNRAS, 342, 725
Diaferio A., Kauffmann G., Colberg J. M., White S. D. M., 1999, MNRAS, 307, 529
Diemand J., Moore B., Stadel J., 2004, MNRAS, 352, 535
Eke V. R. et al. (The 2dFGRS Team), 2004, MNRAS, 348, 866
Ferguson H. C., Sandage A., 1991, AJ, 101, 765
Girardi M., Borgani S., Giuricin G., Mardirossian F., Mezzetti M., 2000, ApJ, 530, 62
Girardi M., Manzato P., Mezzetti M., Giuricin G., Limboz F., 2002, ApJ, 569, 720
Giuricin G., Marinoni C., Ceriani L., Pisani A., 2000, ApJ, 543, 178
Hambly N. C., Irwin M. J., MacGillivray H. T., 2001, MNRAS, 326, 1295
Hoekstra H., Franx M., Kuijken K., van Dokkum P. G., 2002, MNRAS, 333, 911
Hradecky V., Jones C., Donnelly R. H., Djorgovski S. G., Gal R. R., Odewahn S. C., 2000, ApJ, 543, 521
Jenkins A. et al., 1998, ApJ, 499, 20
Kauffmann G., White S. D. M., Guiderdoni B., 1993, MNRAS, 264, 201
Kauffmann G., Colberg J. M., Diaferio A., White S. D. M., 1999, MNRAS, 303, 188
Kneib J.-P. et al., 2003, ApJ, 598, 804
Kochanek C. S. et al., 2001, ApJ, 560, 566
Marinoni C., Hudson M. J., 2002, ApJ, 569, 101
Marinoni C., Hudson M. J., Giuricin G., 2002, ApJ, 569, 91
Norberg P. et al. (The 2dFGRS Team), 2002, MNRAS, 336, 907
Pimbblet K. A., Smail I., Edge A. C., Couch W. J., O'Hely E., Zabludoff A. I., 2001, MNRAS, 327, 588
Press W. H., Schechter P., 1974, ApJ, 187, 425
Ramella M., Pisani A., Geller M. J., 1997, AJ, 113, 483
Sandage A., Tammann G. A., Yahil A., 1979, ApJ, 232, 352 (STY)
Sandage A., Binggeli B., Tammann G. A., 1985, AJ, 90, 1759
Sanderson A. J. R., Ponman T. J., 2003, MNRAS, 345, 1241

Downloaded from https://academic.oup.com/mnras/article-abstract/355/3/769/952880 by California Institute of Technology user on 19 May 2020

Schaeffer R., Maurogordato S., Cappi A., Bernardeau F., 1993, MNRAS, 263, L21
Smith R. M., Driver S. P., Phillipps S., 1997, MNRAS, 287, 415
Spergel D. N. et al., 2003, ApJS, 148, 175
Trentham N., Tully R. B., 2002, MNRAS, 335, 712
Tucker D. L. et al., 2000, ApJS, 130, 237
Tully R. B., 2004, ApJ, in press, (astro-ph/0312441)
White S. D. M., Frenk C. S., 1991, ApJ, 379, 52
Zabludoff A. I., Mulchaey J. S., 2000, ApJ, 539, 136

APPENDIX: CALCULATING GROUP R_F LUMINOSITIES

As the 2dFGRS is a b_J-selected survey, extra consideration is required in order to include the SuperCOSMOS r_F-band data in the analysis. For instance, it is necessary to determine an appropriate local flux limit to which the r_F-band data are complete. The term complete is used here without reference to the well-quantified incompleteness in the redshifts measured for objects in the 2dFGRS parent catalogue, and the possible incompleteness in the parent catalogue itself. A local r_F-band flux limit is determined from the distribution of observed galaxy colours. Fig. A1 shows the cumulative distribution of the galaxy $b_J - r_F$ values for the sets of $z < 0.12$ galaxies in both the mock and the 2dFGRS data. As at least 95 per cent of galaxies are bluer than $b_J - r_F = 1.5$, the local minimum r_F-band flux limit is set equal to $r_{F,lim} = b_{J,lim} - 1.5$. From this figure, one can also infer that the bright $b_J > 14$ limit can essentially be transferred into the r_F band, such that the r_F-band sample is also complete for $r_F > 14$. Thus, a 'complete' r_F-limited sample can be made to a locally defined flux limit corresponding to $14 < r_F < b_{J,lim} - 1.5$. This lower flux limit removes approximately 29 per cent of the galaxies from the sample, whereas only ∼0.4 per cent were discarded for being brighter than the upper flux limit.

Having found flux limits defining a complete r_F-band sample, the intention is, as before, to total the galaxy luminosities, taking into account the weights associated with the redshift incompleteness, and then apply the appropriate Schechter function correction for the galaxies that are too faint to make the flux cut. However, the galaxies included above the r_F flux limit are now a bright subsample of the 2dFGRS parent catalogue. Thus, they are no longer drawn from the same population as the subsample of parent catalogue galaxies without measured redshifts, and so equation (2.2) is no longer an unbiased way to correct for this redshift incompleteness. This complication was sidestepped by redistributing only the weights of galaxies without redshifts and with $14 < r_F < b_{J,lim} - 1.5$. Thus, the subsample of galaxies with redshifts and sufficiently high r_F-band fluxes is now a similar population to those galaxies without redshifts where the weights are redistributed. As only approximately two-thirds of the 2dFGRS galaxies satisfy the r_F flux limits, the weights were redistributed to the nearest seven projected galaxies only. This should match the angular smoothing scale with that used in the b_J band.

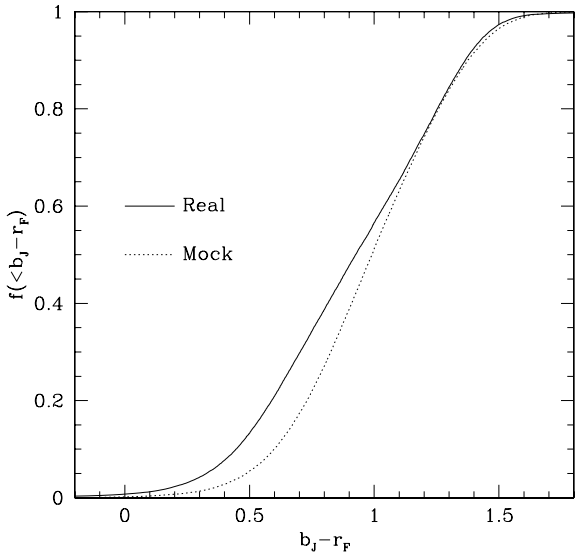

Figure A1. The cumulative distribution of galaxy $b_J - r_F$ values for all $z < 0.12$ galaxies in the 2dFGRS (solid line) and mock (dotted line) catalogues.

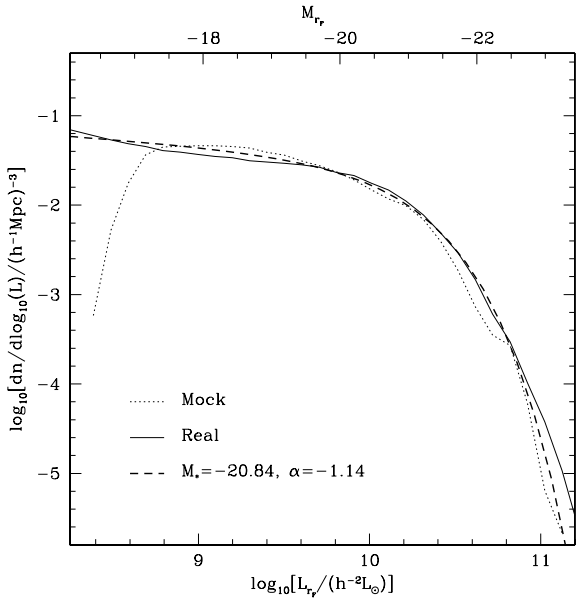

Figure A2. The r_F-band luminosity functions, estimated using a $1/V_{max}$ method, for all $z < 0.12$ galaxies in the mock (dotted line) and 2dFGRS (solid line). The dashed line shows the suitably normalized Schechter function resulting from an STY fit to the 2dFGRS data.

In addition to the correction for redshift incompletion, galaxies below the flux limit also need to be accounted for in determining the total group luminosity. This was accomplished by assuming that the galaxy luminosity function in the groups can be fitted by a Schechter function with $(M_*, \alpha) = (-20.84, -1.14)$. This is the STY-estimated Schechter function for the r_F-band galaxy luminosity function of all $z < 0.12$ galaxies in the 2dFGRS. In calculating this, the following $(k + e)$-correction, derived using Bruzual & Charlot (1993) models, was used:

$$k + e = 0. \quad \text{(A1)}$$

Choosing a normalization to match the luminosity function amplitude inferred using a $1/V_{max}$ estimator leads to $\phi_* = (1.4 \pm 0.1) \times 10^{-2} (h^{-1}\,\mathrm{Mpc})^{-3}$. This value, which neglects the incompleteness in the parent catalogue of the 2dFGRS, gives a mean r_F luminosity density in the Universe of $\rho_{r_F} \approx 2.2 \times 10^8\, h\, L_\odot\, \mathrm{Mpc}^{-3}$. As can be seen in Fig. A2, the r_F-band luminosity functions estimated using the $1/V_{max}$ method are similar in the 2dFGRS and the mock catalogue (which yields $M_* = -20.79$ and $\alpha = -1.17$). For the r_F band, $M_\odot = 4.57$.

This paper has been typeset from a TEX/LATEX file prepared by the author.

Downloaded from https://academic.oup.com/mnras/article-abstract/355/3/769/952880 by California Institute of Technology user on 19 May 2020